SYNTHESIS AND BIOLOGICAL EVALUATION OF AZIDE-TAGGED BIOMIMETIC PROBES FOR GLOBAL LABELING OF THE *SACCHAROMYCES CEREVISIAE* GLYCEROLIPIDOME

A Thesis Presented for the

Master of Science

Degree

The University of Tennessee, Knoxville

Matthew Richard Johnson

December 2020

Copyright © 2020 by Matthew Richard Johnson

All rights reserved.

ACKNOWLEDGEMENTS

I would like to thank Dr. Best for his guidance and mentorship. I have sincerely appreciated your patience, input, and support through the challenges of graduate school. Thank you for ensuring access to funding and materials as well as fostering an atmosphere to grow as a scientist and an individual. To the members of the Best Group past and present: Xiaoyu Xhang, Jinchao Lou, Sara Barker, Christelle Ancajas, Megan Qualls, Ruhani Sagar, and Ryan Fisher, thank you for your support, guidance and friendship. Thank you to my committee members Dr. Tessa Calhoun and Dr. Shawn Campagna for your time, knowledge and feedback. Within the department I would like to thank Lauren Anderson for her example as an instructor. Thank you to Katarina Jones for maintaining the mass spectrometers and assisting with the analysis of the lipid extracts by tandem mass spectrometry. Thank you to the members of the Darko Group: Caleb, Derek, Will, and Anthony for your advice, support, friendship, and laughs; all of which helped me initially decide to attend The University of Tennessee.

Outside of the department I would like to thank Dr. John Dunlap for your guidance with microscopy equipment and support in obtaining images. Thank you to Dr. Todd Reynolds for providing lab space and access to materials to enable all of the cell growth experiments as well as sharing your knowledge and input. I would also like to thank the members of the Reynolds Group for sharing your lab space and helping me with my cell

growth experiments. I especially would like to thank Aeric Zhou for training and assisting me as I work in the lab.

To my undergraduate advisor, Dr. Stephen Chamberland, I would like to say thank you for your continued support and guidance through my academic career and life. I have sincerely appreciated your time and advice. I would not be where I am in my academic career without your support and encouragement. You are an example of the type of educator and scientist that I strive to be. To the rest of my UVU family: Jordan Dickson, Maraia Uluave, and Michael Davenport, thank you for your kindness, friendship, advice, support, and for sharing many laughs and far too many beignets together.

I would like to thank the many members of my family who have loved and supported me throughout my academic career. I love you all. To my grandparents Jean and Gordon Johnson: thank you for always offering a place to get away for the weekend when school was overwhelming as well as great home cooked meals. I sincerely appreciated your helping me adjust to life in Utah as a freshman and for grandpa sitting at the table with me helping me understand calculus. Jeanne and Charles Luker, my Granny and Grampy,: thank you for the years of chess matches, golf outings, and family dinners. We love getting to come visit. To my brother, Tim: thank you for always being there to pick me up when my car broke down and taking the time to help me figure out how to fix it. Thank you for the golf outings to blow off steam and for the late night Beto's runs. To my parents, Richard and Kathee Johnson: I love you both. Thank you for your continued support, guidance and love. Thank you for working though homework

problems on the phone and at the kitchen table. Thank you for making sure we were always able to come home and visit even from Utah.

Sincerely, to my wife, Gina: thank you for being there by my side though everything. There is no way I could have done this without you. Thank you for always being my rock and the ray of hope after every difficult day. Your encouragement, care, and love have meant the most to me. I love you truly. Finally, to my daughter Madeleine: thank you for always running to the door when I get home to exclaim “Daddy!” Watching you grow during these last two years has provided some of the most joyous moments of my life. I love you very much.

ABSTRACT

Lipid metabolism is an extremely complex, interconnected process that, when dysregulated, is strongly linked to cellular disease states including cancer. Study of these metabolic processes is complicated by the characteristic intricacy of these systems; nonetheless, it is achievable through metabolic labeling. Visualization of biosynthesis is an advantage offered by metabolic labeling through the incorporation of fluorescent tags. In this technique, synthetic probes bearing a clickable tag such as azide are fed into live cells where they are directly incorporated using the native enzymatic and cellular processes to metabolically label lipid products. These labeled lipid products are capable of being studied by direct visualization after an alkyne-azide click reaction. The metabolic intermediates of glycerol, monoacylglycerol, glycerol-3-phosphate, and phosphatidic acid were chosen as targets for the development of synthetic probes bearing clickable azide tags due to their central role in lipid metabolism which will be discussed more in the text. Additionally, the azide tag was placed on the glycerol backbone of these metabolic probes to ensure that it is not cleaved during metabolism but can continually be incorporated into a broad range of lipid products for global labeling. Metabolically labeled lipids were evaluated by fluorescence microscopy after a Cu-free click reaction to visualize probe incorporation at the cellular membrane. Fluorescence TLC analysis for visualization of individually labeled lipid products have been conducted with lipid extracts that had been treated with Cu-catalyzed click reaction for incorporation of the fluorescent tag. Efforts to identify and quantify azide-tagged lipid products by HPLC-MS/MS have been initiated.

This thesis describes progress towards the design and synthesis of azide-tagged biomimetic molecular probes and their application toward developing fluorescence labeling via click chemistry as a means for direct imaging and analysis of lipid products.

TABLE OF CONTENTS

Chapter 1. Overview of lipid metabolism and the importance of metabolic labeling in understanding and treating disease 1

1.1. Background 1

1.2. Lipid Metabolism and Disease 7

1.3. Metabolic Labeling 11

1.4. Summary of Project Aims 19

Chapter 2. Azide-Tagged Glycerol-3-Phosphate and Phosphatidic Acid Probes: Design and Synthesis 22

2.1. Probe Design 22

2.2. Results and Discussion 24

2.3. Future Work 28

2.4. Experimental 29

Chapter 3. Azide-Tagged Glycerol and Acylglycerol Probes: Evaluation 32

3.1. Probe Design 32

3.2. Results and Discussion 34

3.3. Future Work 43

3.4. Experimental 44

References 49

Appendix 57

Vita 66

LIST OF FIGURES

Figure 1.1 (a) Generic lipid structure (b) Representative intrinsic curvatures, (c) Lipid self-assembly macrostructures: Inverted Hexagonal Phase (IC < 0); Bilayer and Liposome (IC = 0); Micelle (IC > 0) 2

Figure 1.2 Representative structures of: (a) fatty acids, saturated and unsaturated; (b) glycerolipids; (c) phospholipid structure with headgroup attachment point shown in blue; (d) phospholipid head groups. 4

Figure 1.3 Biological membrane with phospholipids (red outline), proteins (dark blue), cholesterol (light blue), and carbohydrates, glycolipids, and glycoproteins (green)..6

Figure 1.4 Yeast lipid metabolism and selected compounds of interest for metabolic labeling 8

Figure 1.5 Overview of metabolic labeling experiments. 11

Figure 1.6 Overview of click chemistry: (a) Cu-catalyzed click chemistry, (b) Cu-free click chemistry. 14

Figure 1.7 Representations of chemical probes from works of metabolic labeling discussed in this section 16

Figure 2.1 Generic azide-tagged metabolic probe with glycerol backbone in red and azide tag in blue.....22

Figure 2.2 Gly-3-P and PA probes in Chapter 2.....23

Figure 2.3 Synthetic route to N3-Gly-3-P and N3-PA.....25

Figure 2.4 Metal cation induced selectivity for tosylate addition to 1,4-diol[41] 26

Figure 3.1 Representative structures of glycerol-N_3 and 3'-MAG-N_3 probes 32

Figure 3.2 Overview of method for obtaining fluorescent visualization of metabolically labeled cells 36

Figure 3.3 Fluorescence images of *S. cerevisiae* labeled cell culture: control (top) and 3.2 (bottom) 37

Figure 3.4 Fluorescence images of *S. cerevisiae* labeled cell culture.....38

Figure 3.5 Overview of method for obtaining fluorescence TLC of metabolically labeled lipid extracts 41

Figure 3.6 Initial fluorescence TLC images for unlabeled (left) and **3.2** (right).....42

Figure 3.7 Overview of method for mass spectrometry analysis of azide tagged lipid extracts 43

LISTE OF ABBREVIATIONS

AcOH	Acetic Acid
Ag_2O	Silver (I) Oxide
CAC	Citric Acid Cycle
CDCl3	Deuterated Chloroform
CDP	Cytidine Diphosphate
CDP	Cytidine Diphosphate
CH_2Cl_2	Methylene Chloride
$CHCl_3$	Chloroform
CL	Cardiolipin
CMP	Cytidine Monophosphate
CoA	Coenzyme A
CuAAC	Copper catalyzed azide-alkyne cycloaddition
Cy3	Cyanine
DAG	Diacylglycerol
DAG	Diacylglycerol
DBCO	Azadibenzocyclooctyne
DHAP	Dihydroxyacetone Phosphate
DMF	Dimethylformamide
DMSO	Dimethyl Sulfoxide
ER	Endoplasmic Reticulum

Et_3N	Triethyl Amine
EtOH	Ethanol
FA	Fatty Acid
g	Relative Centrifugal Force
G3P	Glyceraldehyde-3-Phosphate
G3P	Glycerol-3-Phosphate
Gly-3-P	Glycerol-3-Phosphate
H_2O	Water
his	Histidine
IC	Intrinsic Curvature
KI	Potassium Iodide
$LiAlH_4$	Lithium Aluminum Hydride
m	meta
M	molar
m-CPBA	*m*-chloroperoxybenzoic acid
MAG	Monoacylglycerol
MeCN	Acetonitrile
MeOH	Methanol
mQ	MilliQ
MS	Mass Spectrometry
mTOR	Mammalian Target of Rapamycin

N_2	Nitrogen Gas
N_3	Azide
Na_2SO_4	Sodium Sulfate
NaN_3	Sodium Azide
o	ortho
OD	Optical Density
p	para
PA	Phosphatidic Acid
PC	Phosphatidylcholine
PCl_3	Phosphorus Trichloride
PE	Phosphatidylethanolamine
PG	Phosphatidylglycerol
PGP	Phosphatidylglycerol Phosphate
PI	Phosphatidylinositol
$PI(3,4,5)P_3$	Phosphatidylinositol-3,4,5-Trisphosphate
PIP_x	Phosphatidylinositol Phosphate
PKC	Protein Kinase C
PLD	Phospholipase D
PS	Phosphatidylserine
Ras	Ras Superfamily of Proteins (**Ra**t **s**arcoma)
rpm	Revolutions per Minute

S. cerevisiae	*Saccharomyces cerevisiae*
sn	Stereospecifically Numbered
TAG	Triacylglycerol
THF	Tetrahydrofuran
TsCl	*p*-toluenesulfonyl chloride
ura	Uracil
WT	Wild Type
x g	Times Gravity
YNB	Yeast Nitrogen Base
YPD	Yeast Extract Peptone Dextrose

CHAPTER 1. OVERVIEW OF LIPID METABOLISM AND THE IMPORTANCE OF METABOLIC LABELING IN UNDERSTANDING AND TREATING DISEASE

1.1. Background

Lipid Structure and Self-Assembly Properties

Due to their amphipathic nature, lipids are the primary components of biological membranes. A generic lipid, illustrated in **Figure 1.1(a)**, is composed of two typical parts: a headgroup that is polar and hydrophilic in nature, and a nonpolar, hydrophobic tail that is made up of alkane and/or alkene hydrocarbon chains. Exclusively alkane hydrocarbon tails are termed saturated and those containing carbon-carbon double bonds are known as unsaturated. The polar headgroups, carbon chain length, and the saturation/ unsaturation of the hydrocarbon tails can vary among different species of lipids, thus influencing the physical characteristics of lipid species and the manner in which individual lipids will interact with each other. This ability of lipids to self-organize in a three-dimensional space is influenced by the intrinsic curvature (IC) of each lipid species, as these structures can have positive, negative or near zero curvature. **Figure 1.1(b)** illustrates the IC of lipids as the following: negative curvature lipids ($IC < 0$) have an inverse cone shape due to a wider tail region than headgroup; those with near zero ($IC = 0$) are

cylindrical in shape due to a roughly equal width of headgroup and tail region; and those with positive curvature are cone shaped due to a wider headgroup versus tail region.[1]

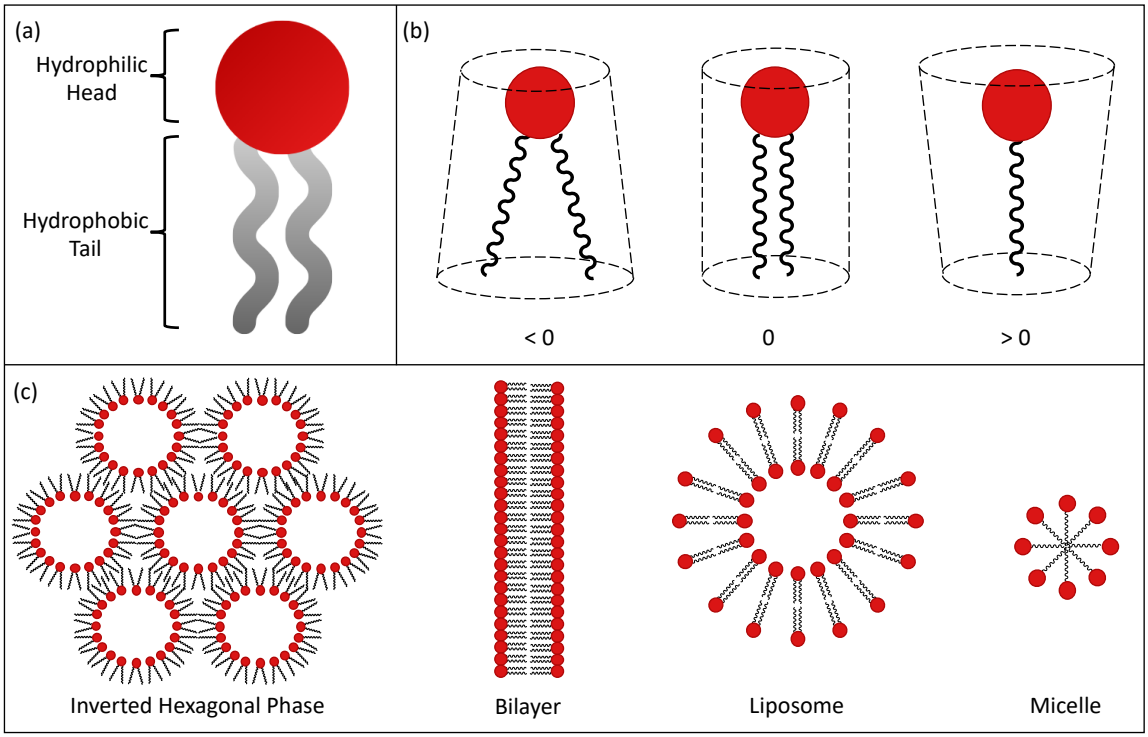


Figure 1.1 (a) Generic lipid structure (b) Representative intrinsic curvatures, (c) Lipid self-assembly macrostructures: Inverted Hexagonal Phase (IC < 0); Bilayer and Liposome (IC = 0); Micelle (IC > 0)

In aqueous conditions, these polar/ nonpolar regions also allow for the self-assembly of lipids into macrostructures as illustrated in **Figure 1.1(c)**. Lipids with negative curvature can form unique structures with the polar head group on the interior of a single unit and the hydrophobic tails on the exterior. Interaction with other units of the same structure contributes to the formation of long, tubular aqueous channels termed the

inverted hexagonal phase. These structures play an important role in the anchoring of G-proteins to the cellular membrane.[2] Bilayers are produced from the assembly of near zero IC lipids into complementary sheets with hydrophobic tails surrounded by polar headgroups on both the exterior and interior surfaces.[3] These bilayers can also form spherical structures termed liposomes containing an aqueous core. This functionality allows for the production of biological membranes necessary for the protection and support of cellular life as well as intercellular transport.[4] Additionally, liposomes are used as drug delivery agents.[5] Micelles are formed as positive curvature lipids aggregate into spherical, monolayer structures with the polar headgroups forming the exterior encompassing the fatty carbon chains at the center.

Lipids Classifications

Lipid species can be divided into classes based on their structure. The simplest lipid forms are fatty acids (FAs) seen in **Figure 1.2(a)**. They can be described by the notation (X : Y), where X refers to the length of the carbon chain and Y indicates the degrees of unsaturation. The length of this alkyl tail varies in observed species; however, physiologically significant fatty acids have a range of about 10-24 carbons in length. The majority of FAs in biology contain even-numbered carbon chains, and these chains may contain a degree of unsaturation up to four.[6] Fatty acids are an important component of glycerolipids, comprising the nonpolar tail region substituted as the acyl chain onto a glycerol backbone. Glycerolipids can be single, double, and triple acyl-chain substituted

at the *sn*-1, *sn*-2, or *sn*-3 positions and characterized as the following: 1- and 2-monoacylglycerols (MAG), diacylglycerols (DAG), and triacylglycerols (TAG), as shown in **Figure 1.2(b)**.

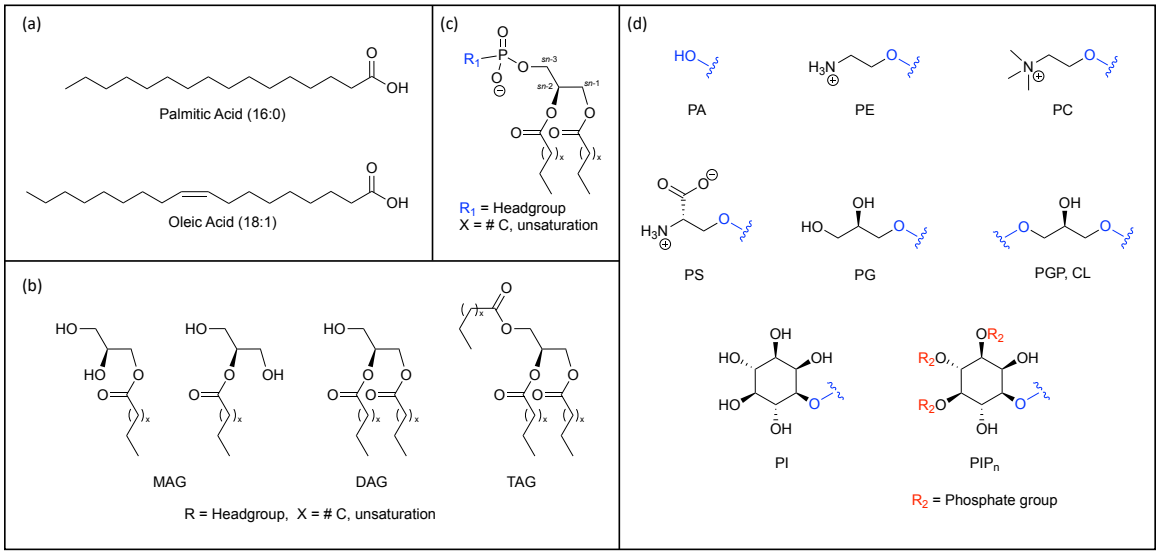


Figure 1.2 Representative structures of: (a) fatty acids, saturated and unsaturated; (b) glycerolipids; (c) phospholipid structure with headgroup attachment point shown in blue; (d) phospholipid head groups.

Glycerolipids can be further specialized into phospholipids by the addition of a phosphate group at the *sn*-3 position with a variable headgroup denoted by the blue R_1 in **Figure 1.2(c)**. **Figure 1.2(d)** outlines the different headgroup structures and how they are attached to the generic phospholipid backbone as the specified R_1 group from **Figure 1.2(c)**. The addition of a hydroxyl group at the R_1 position gives the simplest phospholipid, phosphatidic acid (PA). Similarly, replacement with the following groups gives the corresponding phospholipids: ethanolamine: phosphatidylethanolamine (PE); choline:

phosphatidylcholine; serine: phosphatidylserine(PS); glycerol: phosphatidylglycerol (PG); *myo*-inositol: phosphatidylinositol (PI). Single, double, or triple substitution of the hydroxyl groups on the *myo*-inositol head of PI at the carbon 3, 4, and 5 positions produces the phosphatidylinositol phosphate (PIP_n) family members with n denoting the total number of phosphate groups added to the ring. Similarly, the addition of a phosphate group to the primary alcohol of the glycerol headgroup in PG give phosphatidylglycerol phosphate (PGP). If phosphatidic acid is added to the glycerol headgroup of PG then the phospholipid cardiolipin (CL) is produced. Not only do the phospholipid headgroups identify individual lipid species, each headgroup introduces unique properties such as IC as well as anionic or cationic nature. Most phospholipids are characterized as anionic due to the presence of the acidic phosphate group. However, net neutral phospholipids are represented by PC and PE due to the existence of the positively charged ammonium groups resulting from choline and ethanolamine.

Biological Membranes

Phospholipids are the major components of biological membranes, which are complex systems of many components functioning in cellular structure, messaging, transport, and regulation. As shown in **Figure 1.3**, biological membranes often include elements such as cholesterol, proteins, carbohydrates, and other small molecules in addition to phospholipids to aid in these previously mentioned functions.[7] As phospholipids are a major component, the lipid composition of the membranes is strictly

regulated through cellular metabolism to maintain the appropriate environment.[8] This complex membrane system has not always been clearly understood.

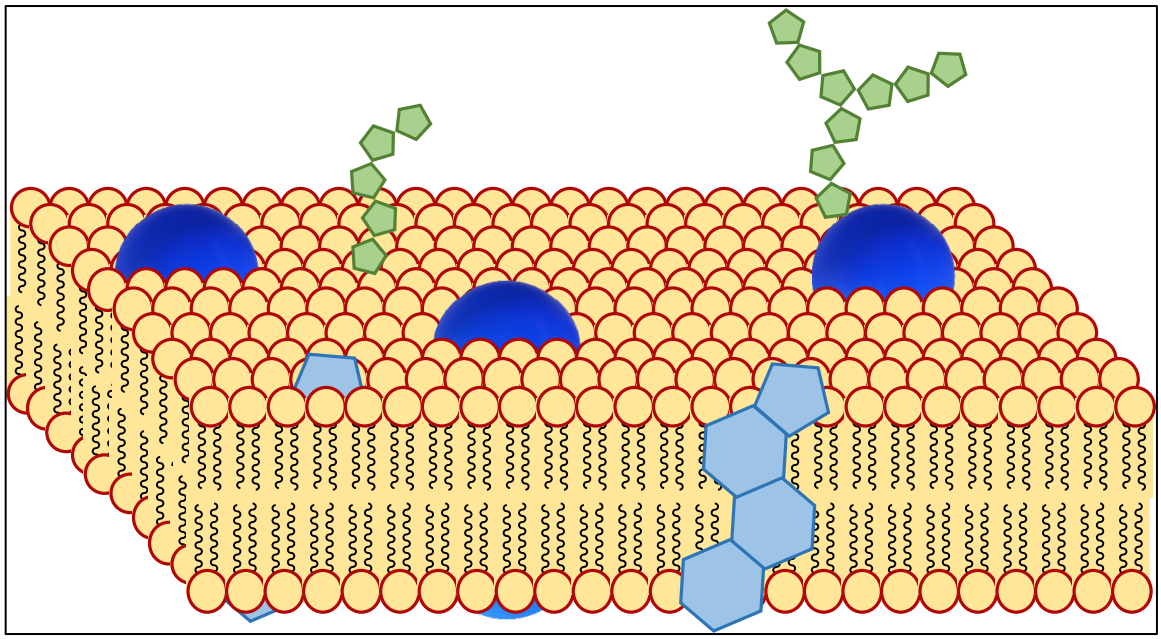


Figure 1.3 Biological membrane with phospholipids (red outline), proteins (dark blue), cholesterol (light blue), and carbohydrates, glycolipids, and glycoproteins (green).

Davson and Danieilli described the biological membrane as a thin lipid film with proteins absorbed onto this film in 1935.[9] While this description allowed for the explanation of cell permeability by the lipid film, it was not a flawless explanation of the presence of proteins at the biological membrane. These ideas were expanded upon by Singer and Nicholson in 1979 with the presentation of the fluid mosaic model of the cell. They proposed that biological membranes are two dimensional solutions in which the lipids and proteins are oriented specifically within the hydrophobic portions of proteins

embedded in the hydrocarbon bilayer and the hydrophilic components are exposed to the aqueous environment.[10] This model was further refined by Simons and Ikonen in 1997, who described the presences of sphingolipids and cholesterol as ordered phases of lipids contrasting with the disordered fluidity of the outer leaflet membrane lipids.[11]

1.2. Lipid Metabolism and Disease

Lipid metabolism is an extremely complex and interconnected system summarized for yeast[12] in **Figure 1.4**. Membrane phospholipids are produced primarily in the endoplasmic reticulum (ER) and the Golgi apparatus of the cell.[13] Glycerolipids are produced beginning from side stream metabolites in glycolysis where glyceraldehyde-3-phosphate (G3P) is converted to dihydroxyacetone phosphate (DHAP), which can then either be acylated to produce MAGs or converted to the synthetic target molecule of **Chapter 2**, glycerol-3-phosphate (Gly-3-P). Gly-3-P can also be produced from glycerol and MAGs, the target molecules of **Chapter 3**. Gly-3-P can then be acylated to give the second synthetic target molecule of **Chapter 2**, phosphatidic acid (PA).

PA is central to lipid synthesis as all other glycerolipids and phospholipids can be produced from this molecule, thus making it a critical synthetic target for this study. To synthesize the other phospholipids, PA is converted to cytidine diphosphate diacylglycerol

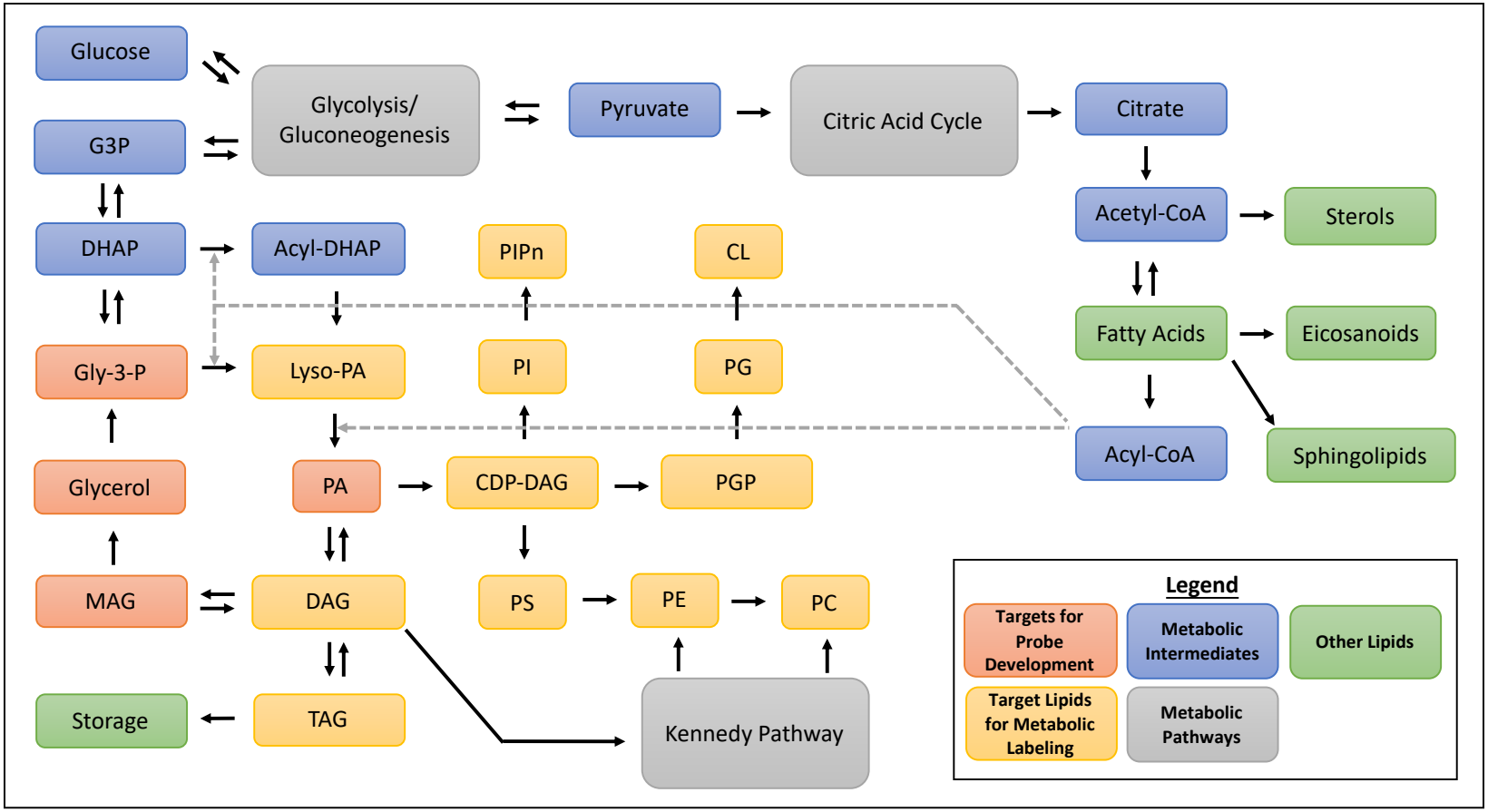


Figure 1.4 Yeast lipid metabolism and selected compounds of interest for metabolic labeling

(CDP-DAG). CDP-DAG is the next crucial intermediate from which the rest of the phospholipids can be produced: it can be converted to phosphatidylinositol (PI) and subsequently phosphatidylinositol polyphosphates (PIP_ns), or it can be converted to phosphatidylserine (PS), which leads to the production of PE and PC. CDP-DAG can also be transformed into phosphatidylglycerol phosphate (PGP), allowing for the production of phosphatidylglycerol (PG) and subsequently cardiolipin (CL). Additionally, PA can be converted to DAG, which can then be acylated to TAG or deacylated to MAG, the synthetic target molecule of **Chapter 3**. DAG can also be transformed into PE and PC via the Kennedy Pathway. This pathway was discovered by Kennedy and Weiss in 1956. They noted that both choline and ethanolamine can be phosphorylated and subsequently cytidine monophosphate can be added to give a high energy cytidine diphosphate (CDP) intermediate. Reaction with DAG gives PE/PC and cytidine monophosphate (CMP).[14]

The synthesis of FAs also plays an important role in lipid metabolism, as these comprise the acyl chains added to DHAP and Gly-3-P. FAs can be produced from pyruvate, another product of glycolysis, which, after entering the citric acid cycle (CAC) and leaving as citrate, is further converted to acetyl-CoA as the building block of fatty acid synthesis. At this point in lipid metabolism, other lipids that are not targets of this study can be produced such as sterols, eicosanoids, and sphingolipids.

Lipid metabolism, while complex, is a tightly controlled network of reactions to maintain the cellular environments and homeostasis.[15] Biosynthesis must also meet the demands for lipids as signaling molecules. The most abundant phospholipid in

eukaryotes[15], PC, is easily hydrolyzed in many signal cascades to PA, DAG, and free fatty acids, thus enabling it to act as a reserve for these signaling lipids.[16] In intracellular signaling pathways, PI acts as a predecessor to second messengers.[17] Lipids can act as enzyme cofactors as in the case of PS, which functions as an activator of protein kinase C (PKC).[18]

MAGs, the metabolic probe target of **Chapter 3**, are well known to have antimicrobial properties and are effective at killing general bacteria, especially *Campylobacter jejuni* but also *Salmonella* and *E. coli*.[19] They were also shown to be particularly effective antimicrobial compounds when added to infant formula.[20] MAGs play a crucial role in mammal immune defense. They act as part of the first line of defense against microbials at the largest barrier of the body, the skin, believed to occur as a gradient throughout the skin.[21] This antimicrobial activity occurs by disruption of the cell membrane or viral envelope by partial dissolution or complete removal of the membrane.[22]

Due to the constant interconversion to other lipids, PA, the target molecule of **Chapter 2**, only accounts for approximately 1% of cellular lipid species. However, PA acts as a lipid second messenger after simple production on demand from PC reserves during hydrolysis by phospholipase D (PLD). It is known that PA binds to and activates proteins such as the mammalian target of rapamycin (mTOR), which suppresses apoptosis in cancer cells.[23] PLD has been associated with most cancers since this enzyme regulates the Ras signaling pathway, which functions in control of cellular propagation, senescence, and

apoptosis, thus strongly linking it to cancer.[24] Notwithstanding the significant role that lipids play in regulation of the cellular environment, tracing these processes is extremely difficult.

1.3. Metabolic Labeling

The goal of metabolic labeling is to incorporate a chemically tagged functionality into a biological system *in vivo* using the biochemical mechanisms of the cellular environment. For the purposes of this study, the integrated chemical tag is an azide

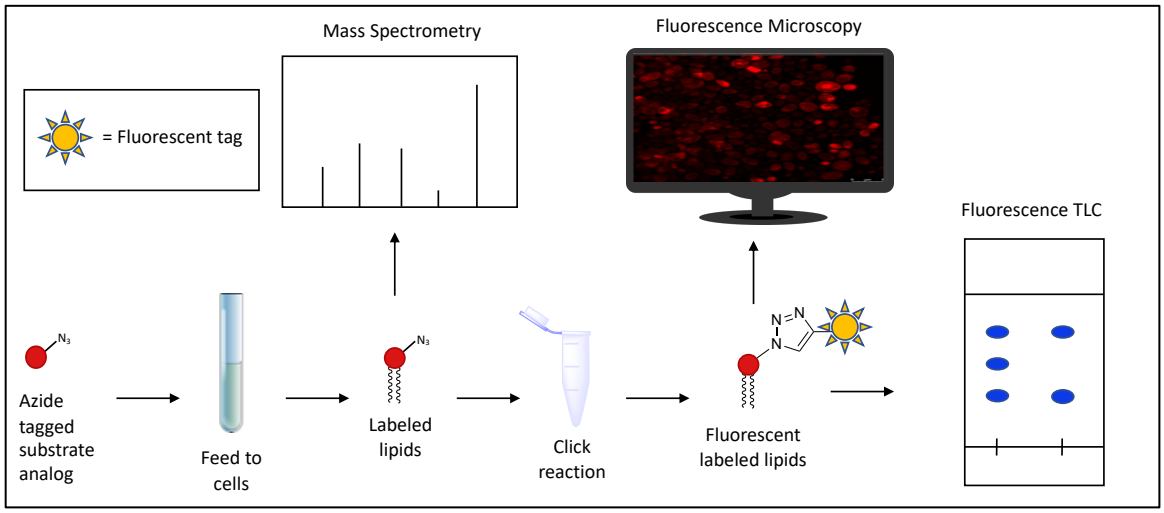


Figure 1.5 Overview of metabolic labeling experiments.

Azide tagged substrate analogs are incorporated into cells in vivo to produce a variety of labeled lipid products. These labeled products can be extracted for analysis by mass spectrometry or a fluorophore can be added via a click reaction (Cu-catalyzed or Cu-free) for analysis by fluorescence microscopy and TLC.

moiety bonded to the glycerol backbone of a glycerolipid analog. Once probe integration has been achieved in vivo during cell culture, it is possible to study the metabolic pathways through which the tag was incorporated by analyzing the labeled cell culture and metabolites. The overall metabolic labeling process is illustrated in **Figure 1.5.** An azide-tagged substrate analog can be fed to live cells where it will be taken up by the cells and used to produce labeled lipid products. These labeled lipid products are then able to be extracted from the cellular environment for quantification and identification by mass spectrometry. Alternatively, reaction via click chemistry, either Cu-catalyzed or Cu-free and illustrated in **Figure 1.6**, incorporates a fluorescent tag to the labeled lipid products through a triazole linkage. These newly fluorescently labeled lipid products can be visualized in vivo by fluorescence microscopy and qualitatively by fluorescence TLC.

History of Metabolic Labeling and Click Chemistry

Metabolic labeling experiments allow for the study, understanding, and eventual contribution toward the treatment of disease states by modifying natural substrates to allow for tracking and study. Traditionally, metabolic labeling has been accomplished by radiolabeling (^{14}C and ^{3}H) metabolite analogs incorporated into biological systems, subsequently studied by scintillation.[25] This approach requires the least modification to the natural chemical structure by simply introducing heavy isotopes. The minimal modification is advantageous in that it helps to ensure labeled metabolites can be easily incorporated into metabolic pathways. While successful, radiolabeling experiments

present many challenges and hazards including safe handling, disposal, and licensing. Previously, this approach was limited in its ability to provide subcellular localization data that is achievable though cellular direct imaging. However, more recent developments have enabled mass spectrometry imaging of lipids.[26] Bertozzi and coworkers produced one of the earliest examples of metabolic labeling through metabolic delivery of ketone-derivatized mannose probes to produce labeled versions of natural sialic acid moieties for the study of cell surface glycoproteins.[27] While this method stepped away from radiolabeling, direct cellular imaging was not achieved though this work.

Subcellular localization of incorporated probes by direct cellular imaging would soon be achievable with the advent of "click chemistry," in which a diverse set of methods for the simplified introduction of carbon-heteroatom-carbon bonds was presented.[28] These reactions allow for the attachment of fluorescent reporter molecules onto the original probe scaffold that has been incorporated in the product substrates by cellular metabolism, thereby allowing for direct cellular imaging by fluorescence microscopy.

The azide moiety is attached onto the probe scaffold to enable post-derivatization via the click reaction. Due to the relatively small size of azide, it is less likely to interfere with the absorption of the probes by the cells and the subsequent production of metabolically labeled products. Copper catalyzed azide-alkyne cycloadditions (CuAAC) and the Cu-free strain promoted cyclooctyne addition are prominent examples of click chemistry that are featured in the biological evaluations of synthetic probes discussed in **Chapter 3**.[29,30] Click chemistry facilitates the cycloaddition of a reactive azide functionality

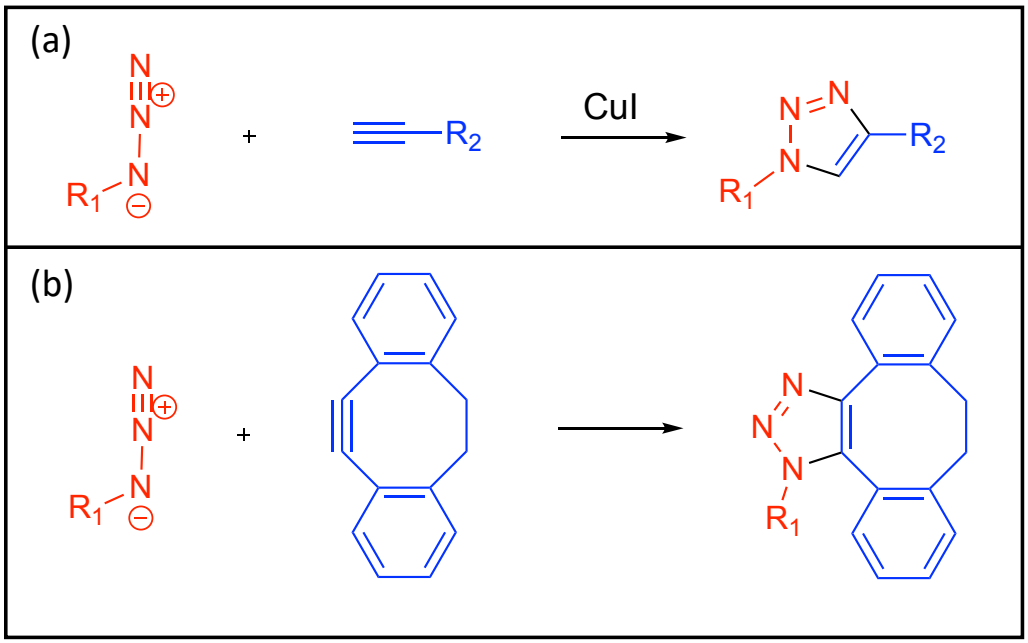


Figure 1.6 Overview of click chemistry: (a) Cu-catalyzed click chemistry, (b) Cu-free click chemistry.

with a terminal alkyne catalyzed by Cu as seen in **Figure 1.6(a)** or the uncatalyzed strain promoted reaction of an azide moiety with a cyclooctyne shown in **Figure 1.6(b)**. In each case the alkyne-containing molecule is bonded to a fluorophore that will ultimately be attached to original azide bearing molecule via a triazole ring.

This mode of labeling is extremely advantageous as it is biorthogonal to the metabolic systems that lead to the eventual labeling of the desired substrates. Allowing this reaction to occur independently of cellular metabolism ensures that all labeled products are produced though the cells own metabolic processes and not due to any external influence. This is essential to this work as all labeling must come though cellular processes to verify the subcellular localization imaging is accurate. Additionally, Cu-free

click-chemistry provides further incentive by removing the need for the toxic Cu catalyst. The click reactions are capable of being performed in ambient conditions and in a modest time period that further highlights the simplicity and effectiveness of the method

Recent Examples of Metabolic Labeling

More recent strategies for metabolic labeling are highlighted in **Figure 1.**7 as a general overview of the different probe designs from the groups discussed in this section. The work of Salic and coworkers in 2009 achieved imageable and traceable metabolic labeling by the incorporation of bio-orthogonal alkyne and azide (N_3) handles for the study of PC. This was accomplished by developing tagged choline analogs of propargyl choline that act as substrates to produce labeled PC products that can then be derivatized with fluorescent click dyes for use in fluorescence microscopy studies for confirmation. These propargyl choline substrates possess a terminal alkyne, that when incorporated into metabolically produced PC can be labeled with a fluorophore via Cu-catalyzed click chemistry. Metabolic labeling was verified by a detergent stain that indicated the presence of propargyl choline in phospholipids. Their presence was further confirmed by diminished staining due to cleavage of the choline head group effected by phospholipase C. Labeling with propargyl choline was shown to be stable with staining occurring around 3-6 hours after addition and lasting beyond 24 hours. Furthermore, labeled PC lipid were shown to reach the outer membrane leaflet by multiple dye staining.[31–33]

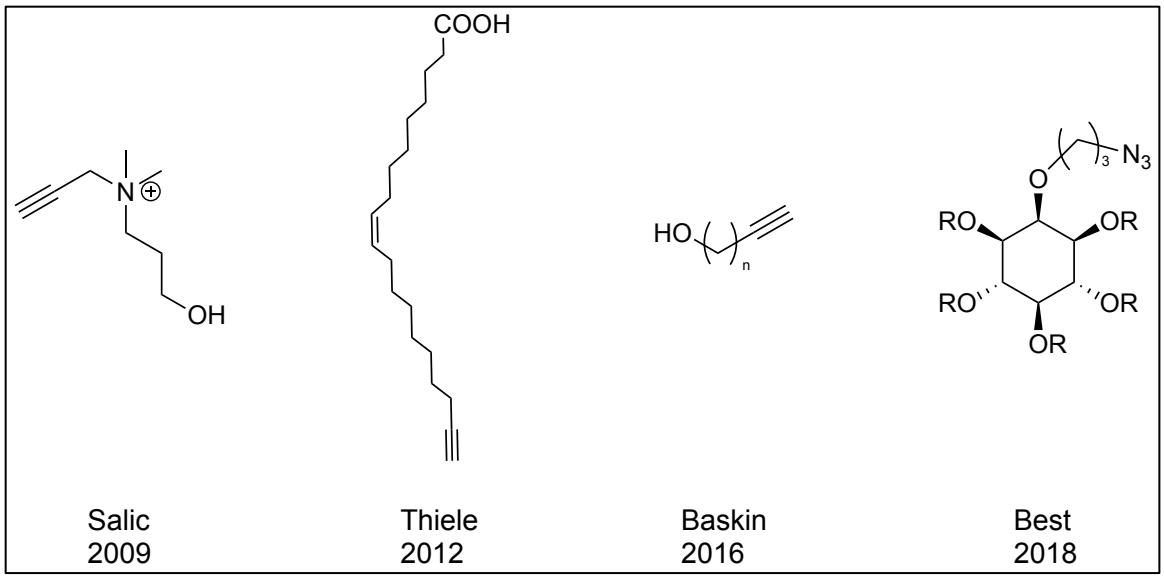


Figure 1.7 Representations of chemical probes from works of metabolic labeling discussed in this section

Salic 2009: alkyne-tagged propargyl choline for labeling PC; Thiele 2012: alkyne tagged oleate for labeling phospholipids produced by FAs; Baskin 2016: alkynol for labeling PA synthesis; Best 2018: azide tagged *myo*-inositol for study of PI.

Thiele similarly studied FA metabolism in 2012 via click alkyne tags attached to multiple saturated FA probes along with an alkyne-tagged oleate probe, since oleate is one of the most prevalent FAs in nature. These FA probes were fed to live cell cultures, which were then harvested after incubation and the lipids were extracted for analysis of the labeled lipid products. The lipid extracts were then clicked with a fluorogenic azide dye that is not fluorescent before the click reaction but forms a fluorescent compound after clicking with a terminal alkyne tag. At this point in the study, the clicked lipid extracts were separated on TLC while compared against lipid standards synthesized with an alkyne oleate for accurate comparison. Labeled products showed similar separation on TLC

compared to the synthesized standards. These results were also compared with ^{3}H-labeled FAs that showed comparable results. This method was again advantageous over classic radiolabeling due to lack of specialized equipment, handling procedures, and shorter development times for TLC imaging. Fluorescence TLC is also cheaper and simpler than separation and analysis by mass spectrometry. However, this method is lacking in the resolution for separated lipids on TLC that can be accomplished by mass spectrometry.[34]

Thiele followed up on this work in 2013 with alkyne labeling on the acyl chain of lipids that could be used in conjunction with click chemistry for in vitro assays to characterize lipid metabolism enzymes. Assays for lysophosphatidic acid acyl transferase, lysophosphatidylcholine acyl transferase, and ceramide synthase with an alkyne-sphinganine were all evaluated for Michaelis Menten kinetics. The results showed no shift in the Michaelis Menten curve indicating that alkyne labeled lipids are effective substrates for in vitro enzymatic assay analysis. Drawbacks to this method are similar to those previously mentioned: high resolution must be achieved by mass spectrometry. Additionally, not all enzymatic assays are capable of being evaluated with this technique involving a terminal acyl chain alkyne. The label is lost during β-oxidation of FAs as well as by the cleavage of the PC headgroup choline by Phospholipase D to give PA.[35]

In 2015, Guo succeeded in labeling glycosylphosphatidylinositol anchors with a fluorescent reporter molecule through a Cu-catalyzed azide click reaction for installation of a biotin derivative fluorescent reporter. This advancement was significant as it was an

additional strategy for phospholipid headgroup labeling comparable to the work Salic in 2009. This work allows for the visualization of glycosylphosphatidylinositol anchorages and studying the effect of the structure on biological function.[36]

Baskin accomplished fluorophore labeling of PA for cellular visualization by producing alkyne-tagged PA analogs clicked by CuAAC. This was achieved by exploiting the fact that PLD not only catalyzes the conversion of PC to PA by cleavage of the choline headgroup but can also facilitate transphosphatidylation reactions to incorporate short chain primary alcohols at the phosphate head. Therefore, Baskin and coworkers selected short chain alkynols for incorporation onto the phospholipid structure. Imaging of PA synthesis was accomplished by treating HeLa cells with these short chain alkynols in vivo. The cells were then subjected to Cu-catalyzed click conditions (CuAAC) for fluorescent tag addition. Subcellular localization of PA was reported at the cellular membrane, Golgi apparatus, and Endoplasmic reticulum coinciding with data reported for the localization of PLD.[37]

Additionally, the Best Group achieved labeling of phosphatidylinositol lipid products through a *myo*-inositol probe shown in **Figure 1.**7 which also contains representations of the other probes discussed in this section, excluding the work or Guo and coworkers. The R groups on the *myo*-inositol probe can be either all hydrogen atoms or all acetyl groups. This specific probe features an additional three carbon chain by which the azide tag is attached to *myo*-inositol 2-position. Once the *myo*-inositol probes were produced, they were fed to live cells to be incorporated into phospholipids though

metabolic labeling. The labeled lipid products were then studied by fluorescence microscopy after a Cu-free click reaction to add a fluorescent tag to verify incorporation into cells. After verification of metabolism of the probes, the labeled lipids could be studied by fluorescence TLC. The spots produced from labeled lipid products were very similar to those of the standards. The labeled lipid extracts were also studied by mass spectrometry where several different azido-PI products with acyl chains of varying lengths were identified. .[38]

1.4. Summary of Project Aims

Inherent to metabolic labeling experiments is the challenge to selectively label desired downstream targets. This is abundantly evident in lipid metabolic labeling experiments due to the complexity and fundamental interconnections intermediates in the lipid metabolic pathway. Some experiments can control downstream labeling of metabolites by placing the functional handle on a specific phospholipid headgroup precursor, limiting the labeling to the scope of the tagged precursor. However, this can make the labeling of some lipids more challenging by reducing the ability to incorporate the labeled headgroup. This method also does not allow for metabolic labeling of glycerolipids since they do not have the phospholipid headgroup attached. Alternatively, if the label is applied at the acyl chain, no mechanisms exist to prevent interconversion and subsequent incorporation of the tag at various phospholipids, glycerol lipids, fatty

acids, eicosanoids, and sphingolipids. Therefore, the location of the function handle should be chosen appropriately to facilitate the desired outcome.

Rather than contend with the natural metabolic processes, this project seeks to exploit the complexity of lipid metabolism to achieve the global labeling of the *Saccharomyces cerevisiae* (*S. cerevisiae*) glycerophospholipid lipidome. Global labeling could be used to further elucidate lipid metabolism and enhance the understanding of altered glycerolipid biosynthesis in cancer cells in terms of synthesis and subcellular localization as a result of the diseased state. This enhanced understanding would hopefully also lead toward improved detection and treatment of cancer.

Two classes of probes have been selected to achieve the project aims: phosphoglycerol based probes discussed in **Chapter** 2 and acylglycerol probes discussed in **Chapter 3**. These probes were chosen because they are natural precursors to all phospholipids and glycerolipids. Due to the central role of PA in the metabolism of lipids, this project seeks to design and synthesize the following biomimetic probes: azide-tagged phosphatidic acid (N_3-PA) and azide-tagged glycerol-3-phosphate (N_3-Gly-3-P), a precursor to PA, through chemical synthesis. Once produced, these probes will undergo biological evaluation studies to confirm incorporation, cell viability, and identification of the metabolites into which the tag was integrated. This will be accomplished by fluorescence microscopy, florescence TLC, and MS experiments. Yeast was chosen as the experimental organism for its simplicity to handle and quick growth as well as the evolutionary conservation of lipid metabolism amongst eukaryotes.[39] Additionally,

acylglycerol probes previously synthesized by Adam Carr in the Best group will undergo these same biological evaluations.

CHAPTER 2. AZIDE-TAGGED GLYCEROL-3-PHOSPHATE AND PHOSPHATIDIC ACID PROBES: DESIGN AND SYNTHESIS

2.1. Probe Design

The specific analogs of Gly-3-P and PA were chosen as the synthetic targets for this study due to their central role in lipid metabolism as precursors to all phospholipids. As illustrated in **Figure 2.1**, the clickable azide handle (blue) is attached to the glycerol backbone (red) via a methyl spacer group. Because the handle is attached to the glycerol backbone, it will continually be associated with all glycerol-based intermediates, including phospholipids, during cellular metabolism thus enhancing global labeling.

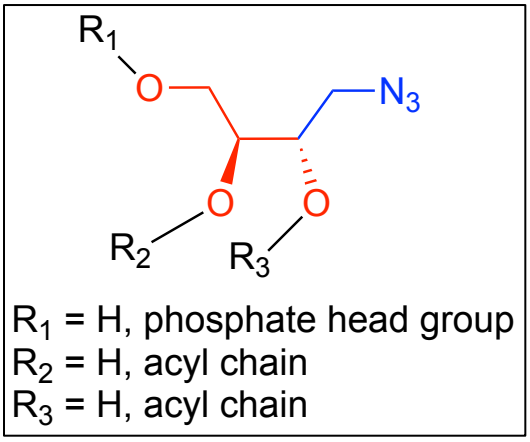


Figure 2.1 Generic azide-tagged metabolic probe with glycerol backbone in red and azide tag in blue

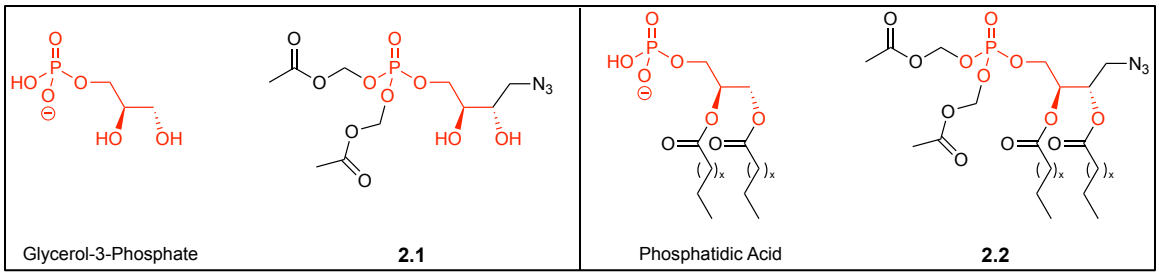


Figure 2.2 Gly-3-P and PA probes in Chapter 2

Due to the relatively small size of the azide moiety, it is expected that this will not interfere with cellular uptake and metabolism of the designed probes. Furthermore, our group has previously shown that PA probes containing azidomethylene at *sn*-3 position are still recognized by PA-binding proteins.[40] Therefore, N_3-Gly-3-P (**2.1**) and N_3-PA (**2.2**), shown in **Figure 2.2** along with their natural underivatized counterparts of glycerol and MAG, were envisioned as ideal candidates for global labeling of lipid products. To facilitate the desired result of global labeling, each probe contains an azide clickable tag attached to the glycerol backbone. It is believed that this design will ensure that, when taken up by the enzymatic machinery of the cell, the probe can be metabolized into all glycerolipid products by maintaining its position anchored to the glycerolipid backbone. This is significant since if the azide tag were attached to the phosphate head group or the acyl chain, it could easily be cleaved by many cellular metabolic processes and could not achieve the desired effect of global labeling. As probe **2.2** only differs from **2.1** by the addition of acyl carbon chains, following successful synthesis of **2.1**, probe **2.2** can be produced by the addition of FA chains.

2.2. Results and Discussion

The synthetic scheme for the production of the azide-tagged target molecules can be seen in **Figure 2.2**. Gly-3-P and PA target analogs were synthesized beginning with commercially available diethyl-L-tartrate, **2.3**. The addition of cyclopentanone in toluene with an acid catalyst produced the protected tartrate **2.4**. With the protected tartrate **2.4** in hand, the ester groups were reduced by $LiAlH_4$ in anhydrous THF under N_2 overnight to produce the 1-4-diol **2.5**.[40] This reaction gave significant issues initially with no conversion of the starting material at various equivalents of $LiAlH_4$ up to 10. It was concluded that the store of hydride reagent was no longer functional. Upon replacement with fresh $LiAlH_4$, the reaction repeatedly produced the desired product in greater than 60% yield.

Once the ester groups had been reduced, the N_3 tag was ready to be installed. A previously published procedure was followed by suspending the newly formed **2.5** in CH_2Cl_2 and adding Ag_2O, TsCl, and KI with stirring at room temperature for 2 hours.[40] This reaction also gave significant issues as multiple attempts at following the procedure failed to produce the desired azide substituted product. Endeavors were made to isolate the tosylated intermediate in step one of the reaction but, after careful analysis, it was

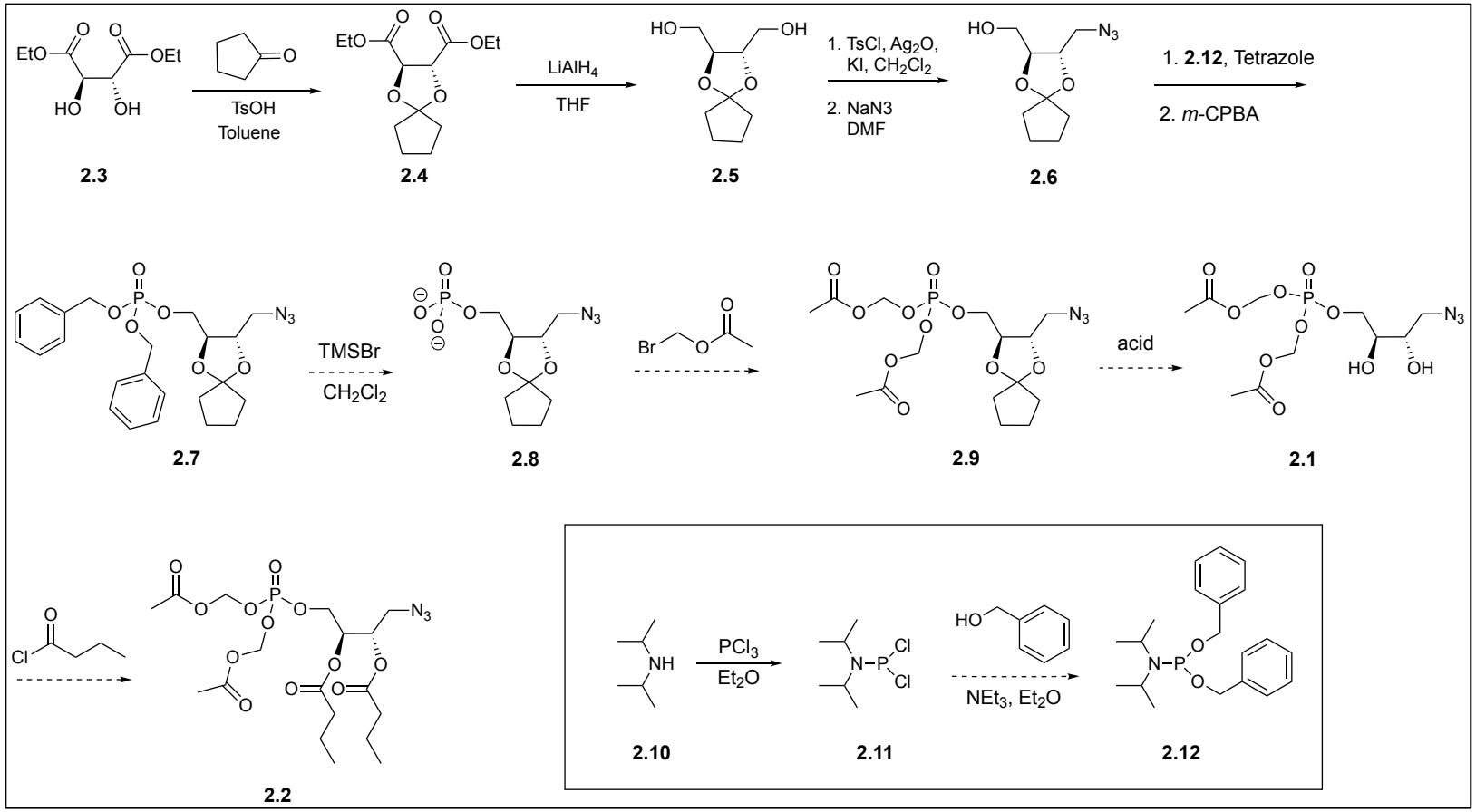


Figure 2.3 Synthetic route to N3-Gly-3-P and N3-PA

concluded that the tosyl group was not adding to the diol. To potentially remedy this issue, an effort was made to install the tosylated intermediate by using Et_3N to maintain basic conditions during addition of the tosyl group and allow for subsequent substitution of the azide in step two, illustrated in **Figure 2.3**. However, this proved to be unsuccessful as this reaction appeared to produce both mono- and di-tosylated products due to a lack of selectivity.

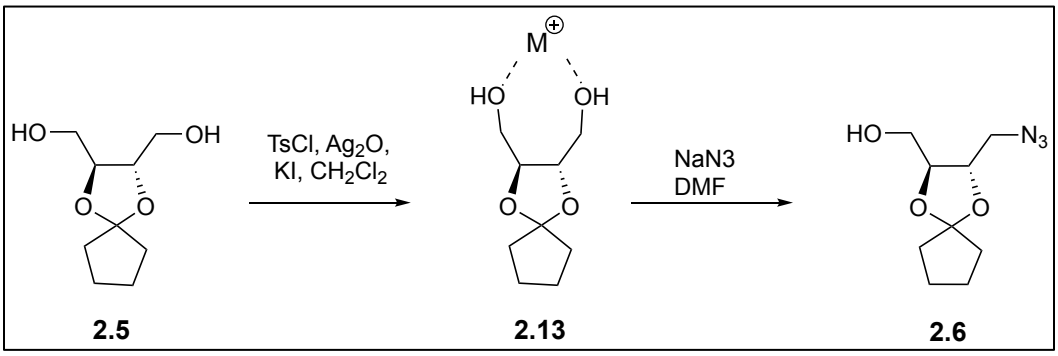


Figure 2.4 Metal cation induced selectivity for tosylate addition to 1,4-diol[41]

Consequential to this over addition, the original strategy was revisited. **Figure 2.4** outlines the importance of the silver (I) oxide in the reaction as it acts to tie up the 1-4-diol, bringing both hydroxy groups into the same conformation and favoring mono-tosylation to occur. Believing this to be the best strategy, an earnest effort was made to discover the source of difficulty for this reaction. Upon carefully reviewing and analyzing each reagent it was discovered that the bottle of silver oxide reagent being used was predominantly silver (II) oxide. After securing a source of only silver (I) oxide, the reaction

proved successful at first glance. Preliminary analysis by NMR showed the expected chemical shifts present. However, the spectra contained significant peaks in the aromatic region leading to the belief that tosyl chloride remained present in the sample. This was further evidenced by the expected integration not matching previous reports while the expected chemical shifts were present.

While working toward the successful installation of the azide handle, attempts were made to synthesize the needed phosphoramidite reagent **2.12**. *N*,*N*-diisopropylphosphoramide dichloride (**2.11**) was produced by the addition of PCl_3 to diisopropyl amine in Et_2O.[42] To ensure success of this reaction, PCl_3 was carefully distilled and used immediately. While the production of **2.11** was effective and straightforward, synthesis of *N*,*N*-diisopropyl dibenzyl phosphoramidite (**2.12**) proved unsuccessful. Benzyl alcohol was added to **2.11** in the presence of Et_3N and Et_2O.[43] After multiple attempts to produce **2.12**, phosphorus was not found in the product of the reaction. This was in contrast to **2.11** were the presence of phosphorus had been verified by ^{31}P NMR spectroscopy. Efforts to vary the solvent, temperature, and reaction time all proved unsuccessful in the effort to produce the desired phosphoramidite. With several failed attempts at the synthesis of **2.12** and the successful addition of the azide handle to the glycerol backbone, the decision was made to abandon attempts to produce **2.12** and use a commercially purchased phosphoramidite. Next, with the azide group successfully installed, the synthesis was primed to introduce the phosphate group by addition of *N*,*N*-

diisopropyl dibenzyl phosphoramidite to give **2.7**. The initial attempt of the addition of the phosphate group proved to be unsuccessful.

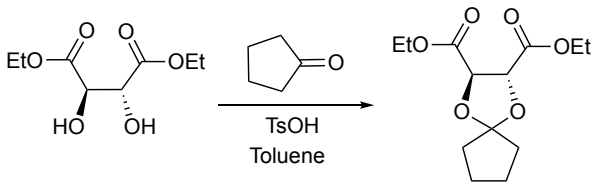
2.3. Future Work

The clickable azide tag was successfully introduced to the glycerolipid backbone. It was determined that only silver (I) oxide mediated tosyl addition will allow for the monotosylation necessary to install the individual azide tag. However, a pure NMR spectra was unable to be obtained due to issues during the purification process. The NMR spectra showed expected peaks for the azido-alcohol compound **2.6**, but also contained significant aromatic peaks leading to the belief that tosyl chloride was still present in the sample. Further purification of **2.6** is required before proceeding on with the synthesis. Completion of the synthetic remaining route is required prior to any biological evaluation. The proposed remaining synthetic route consists of addition of the phosphate group with *N*,*N*-diisopropyl dibenzyl phosphoramidite and 1H-Tetrazol followed my *m*-CPBA to give **2.7**. Removal of the benzyl protecting groups with TMSBr is expected to give **2.8**, which is immediately ready to be protected with dimethyl acetate, producing **2.9**. Finally, acetal deprotection can afford N_3-Gly-3-P (**2.1**), which can be acylated to give N_3-PA (**2.2**), both of which will be evaluated for metabolic labeling. Acyl chains of varying lengths and degrees of saturations can be used to produce multiple analogs of **2.2** for study.

After synthetic production, both N_3-Gly-3-P (**2.1**) and N_3-PA (**2.2**) can be added to cell culture in vivo for incorporation into the cellular biomembranes though metabolic

labeling. The whole labeled cells can be visualized thought Cu-free click chemistry and fluorescence microscopy. Cell viability studies will be performed to quantify the toxicity of each labeled probe on a growing cell population. Labeled content of lipid extracts can be identified via Cu-catalyzed click chemistry for fluorescence TLC. Tandem mass spectrometry can also be used to identify and quantify the labeled lipid product. Labeling validation by in-vitro assays can also be used to confirm metabolic labeling.

2.4. Experimental

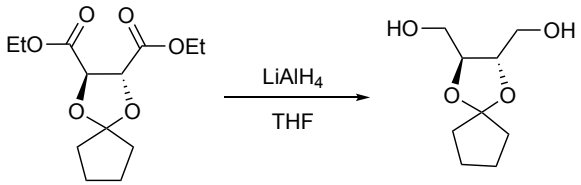


2.3 **2.4**

Diethyl (2R,3R)-1,4-dioxaspiro[4.4]nonane-2,3-dicarboxylate

To a 250 mL round bottom flask with stir bar was added diethyl-L-tartrate (0.83 mL, 1.00 g, 4.85 mmol) dissolved in 40 mL of toluene. Next, cyclopentanone (2.15 mL, 2.04 g, 2.14 mmol) and *p*-toluene sulfonic acid monohydrate (0.09 g, 0.49 mmol) were added and a Dean-Stark trap was attached. The mixture was stirred overnight at 130 °C. After stirring, the reaction mixture was cooled to room temperature and sodium bicarbonate (0.07 g, 0.97 mmol) was added. The resulting mixture was stirred for 10 minutes after which it was gravity filtered and concentrated in vacuo. Flash column chromatography on silica gel with a gradient solvent system of 0-20% ethyl acetate to hexanes afforded protected

tartrate as a yellow oil (1.064 g, 3.910 mmol, 80.6%): ^{1}H NMR (300 MHz, $CDCl_3$) δ 4.73 (s, 2H), 4.27 (q, J = 7.1, 0.6 Hz, 4H), 2.05 – 1.80 (m, 4H), 1.76 – 1.67 (m, 4H), 1.37 – 1.26 (t, J = 7.2 MHz, 6H); ^{13}C NMR (75 MHz, CDCl3) δ 169.8, 123.5, 77.1, 62.0, 36.7, 23.6, 14.3; HRMS $[M + H]^+$ calculated: 273.13381, found: 273.11060.[40]



2.4 **2.5**

((2S,3S)-1,4-Dioxaspiro[4.4]nonane-2,3-diyl)dimethanol

To an oven dried 250 mL round bottom flask with stir bar under N_2 was added **2.4** (1.502 g, 5.513 mmol), which was then dissolved in 20 mL dry THF. The solution was cooled to 0 °C upon which $LiAlH_4$ (0.628 g, 16.539 mmol) was added carefully to the flask. The reaction mixture was stirred for 10 minutes at 0 °C, warmed to room temperature and stirred overnight, then cooled again to 0 °C and stirred 10 minutes. Carefully, H_2O was added dropwise to quench. Na_2SO_4 was added to remove H_2O and the mixture was stirred 15 minutes upon which it was filtered through a plug of celite washing with acetone. Na_2SO_4 was again added to ensure the removal of all H_2O upon which the product was concentrated in vacuo. Flash column chromatography on silica gel with a gradient solvent system of 50-100% ethyl acetate to hexanes afforded diol **2.5** as a yellow oil (0.703 g, 3.732 mmol, 67.7%): ^{1}H NMR (300 MHz, $CDCl_3$) δ 3.98 – 3.94 (m, 2H), 3.84 – 3.66 (m, 4H),

2.04 – 1.95 (m, 2H), 1.92 – 1.75 (m, 4H), 1.74 – 1.61 (m, 4H); ^{13}C NMR (75 MHz, CDCl3) δ 211.7, 77.1, 62.8, 38.0, 24.0; HRMS $[M + H]^+$ calculated: 189.11268, found: 189.07753.[40]

CHAPTER 3. AZIDE-TAGGED GLYCEROL AND ACYLGLYCEROL PROBES: EVALUATION

3.1. Probe Design

The azide-tagged glycerol and 3'-monoacylglycerol probes in this chapter are represented by the structures shown in **Figure 3.1**. These probes share in common a glycerol backbone, highlighted in red, with the necessary azide functionalization for metabolic labeling in black. The length and unsaturation of the acyl carbon chain attached at the R position of all 3'-MAG-N_3 varies among probes. **Table 3.1** contains gives of the names of varying ester carbon chain lengths and unsaturation and the corresponding unique compound number for each metabolic probe.

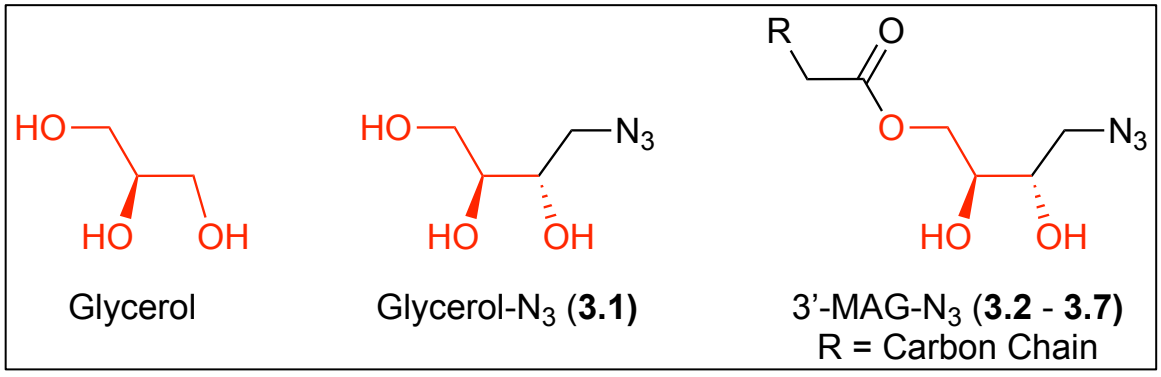


Figure 3.1 Representative structures of glycerol-N_3 and 3'-MAG-N_3 probes

Table 3.1 Names, acyl carbon chain length and unsaturation corresponding to 3'-MAG-N_3 probes

Ester Carbon Chain Name	Number of C & Unsaturation	Compound Number
Capryl	(10:0)	**3.2**
Lauryl	(12:0)	**3.3**
Myristoyl	(14:0)	**3.4**
Palmitoyl	(16:0)	**3.5**
Steroyl	(18:0)	**3.6**
Oleoyl	(18:1)	**3.7**

The design of the probes in this chapter was influenced by the relative simplicity of the glycerol and MAG structures as well as the fact that glycerol and MAGs are significant central intermediates of lipid metabolism. It is expected these probes will label a wide array of phospholipid and glycerolipid products. This is believed to be the case due to the ability of glycerol and MAGs to be converted to PA, the central intermediate, by cellular mechanisms as show in **Figure 1.5**. Due to the relatively small nature of the incorporated azide tag, these probes should be easily absorbed by the cells and incorporated into lipid metabolism for labeling downstream lipid products. If conversion to PA is successful, it is expected that the incorporated probes can be functionalized into the remaining phospholipid species as well as DAG and TAG. Additionally, 3'-MAG-N_3 probes were developed to help ensure labeling of DAG and TAG metabolites by blocking

the *sn*-3 position. With the phosphate headgroup blocked from bonding to this position of the glycerol backbone, at minimum labeling of DAG and TAG would be expected to be observed. However, DAG can still be converted to phospholipids and thus labeling of glycerophospholipids is also expected with these probes. All metabolic probes in this chapter were synthesized previously by Dr. Adam Carr of the Best Group.[44]

3.2. Results and Discussion

Incorporation the azide-tagged probes was accomplished by directly feeding the probes into live cells for processing and labeling of other lipid products by the cellular metabolic pathways. Due to the small size of the biorthogonal azide handle, it is believed that glycerol-N_3 and 3'-MAG-N_3 probes should participate in cellular metabolic process for downstream labeling of phospholipid and glycerolipid molecules. Additionally, due to the centrality of the probes in lipid metabolism, it is expected that labeling a wide range of lipid products should occur easily.

Metabolic labeling experiments were conducted to verify incorporation and effectiveness of the azide-tagged molecular probes into different glycerolipid products in *S. cerevisiae* cellular cultures. The yeast strain was streaked onto a YPD plate and allowed to grow for 24 hours before initiating liquid based media growth experiments. Plates were stored for up to two weeks in the freezer. A loop of cells was inoculated into a 2% galactose minimal media solution where the cells were allowed to grow overnight. The following day, the cell cultures were spiked with a 50 μM final concentration of the

appropriate molecular probe. The cells were again allowed to grow overnight in support of full incorporation of the probe by the cells to allow for metabolic labeling. After the cellular growth phase was complete, the cells were washed and spun down in the centrifuge to either be used immediately or stored in the freezer.[45] Once labeled, the cells were ready for analysis by three different techniques: fluorescence microscopy, fluorescence TLC, and tandem LC-MS spectroscopy. All cell growth and metabolic labeling experiments were performed in the laboratory of Dr. Todd Reynolds – Department of Microbiology, The University of Tennessee, Knoxville with the assistance of his graduate student, Yue "Aeric" Zhou.

Fluorescence Microscopy

Fluorescence microscopy allows for the imaging of fluorescently tagged molecules and subsequently the visualization of the subcellular localization of the metabolically incorporated probe. The production of azide-tagged lipid products from the probes allows for the derivatization through Cu-free click chemistry to introduce fluorescent tags to the previously metabolically labeled cells. This was accomplished by incubating the cells with the cyclooctyne dye, DBCO-Cy3. The fluorescently tagged cells were then washed to remove any residual dye and lower the possibility of background fluorescence. An aliquot of labeled cells was place onto a microscope slide with coverslip and visualized before drying.[46]

An overview for the process of metabolic labeling to visualize fluorescently tagged cells via fluorescence microscopy is provided in **Figure 3.2**. The synthetic, azide tagged glycerol and MAG probes were fed to cells in vivo for incorporation directly though natural cellular process due to the overall similar structure of the probes to their natural analogues. After incubation, the cells were harvested, washed, and spun down to be used immediately or stored in the freezer at -80 °C for later use.

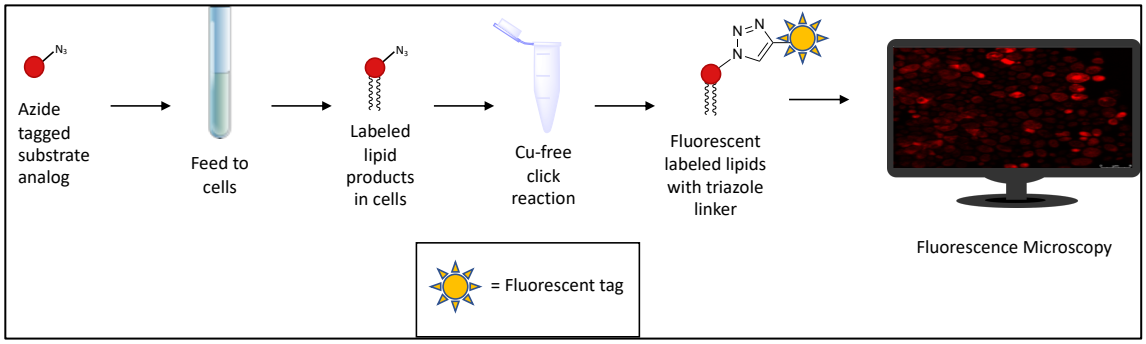


Figure 3.2 Overview of method for obtaining fluorescent visualization of metabolically labeled cells

Fluorescent tags were then added directly to the cell culture by Cu-free click chemistry through the strain promoted reaction of the cyclooctyne Cy3-DBCO with the installed azide functionality. After incubation with the dye the cell cultures underwent various washing procedures to ensure removal off any excess dye to limit background noise in the images. At this point, droplets of the cell cultures we fixed onto microscope slides and visualized by fluorescence microscopy. All fluorescence microscopy images were captured on an SP8 White Light Laser Confocal System at the Advanced Microscopy

and Imaging Center – The University of Tennessee, Knoxville. Fluorescence images and white light images were both captured and can be analyzed side by side and overlaid. This allows for better visualization of the control cells, unlabeled, as they do not fluoresce but can be seen as present.

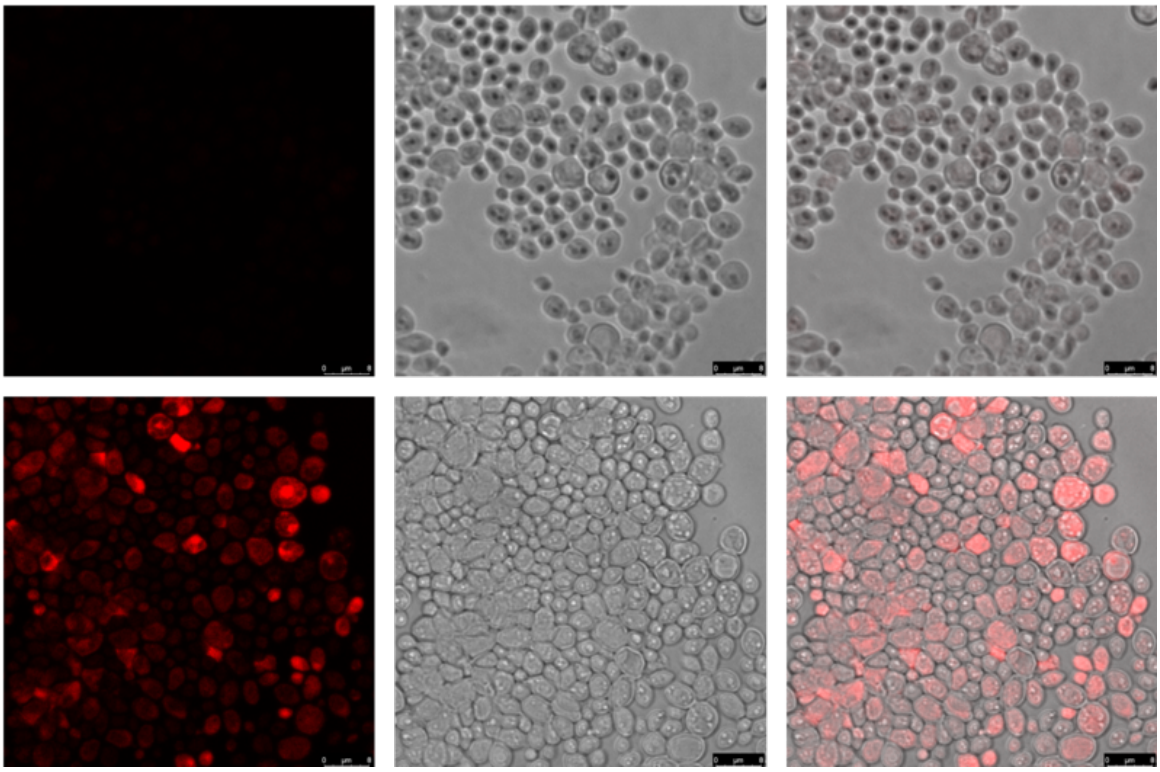


Figure 3.3 Fluorescence images of *S. cerevisiae* labeled cell culture: control (top) and 3.2 (bottom)

Scale bars 8 μm

Based on encouraging results from prior work by Dr. Carr, compound **3.2** was selected to commence metabolic labeling studies. Initially, labeling proved to be challenging as preliminary control images contained a significant amount of background

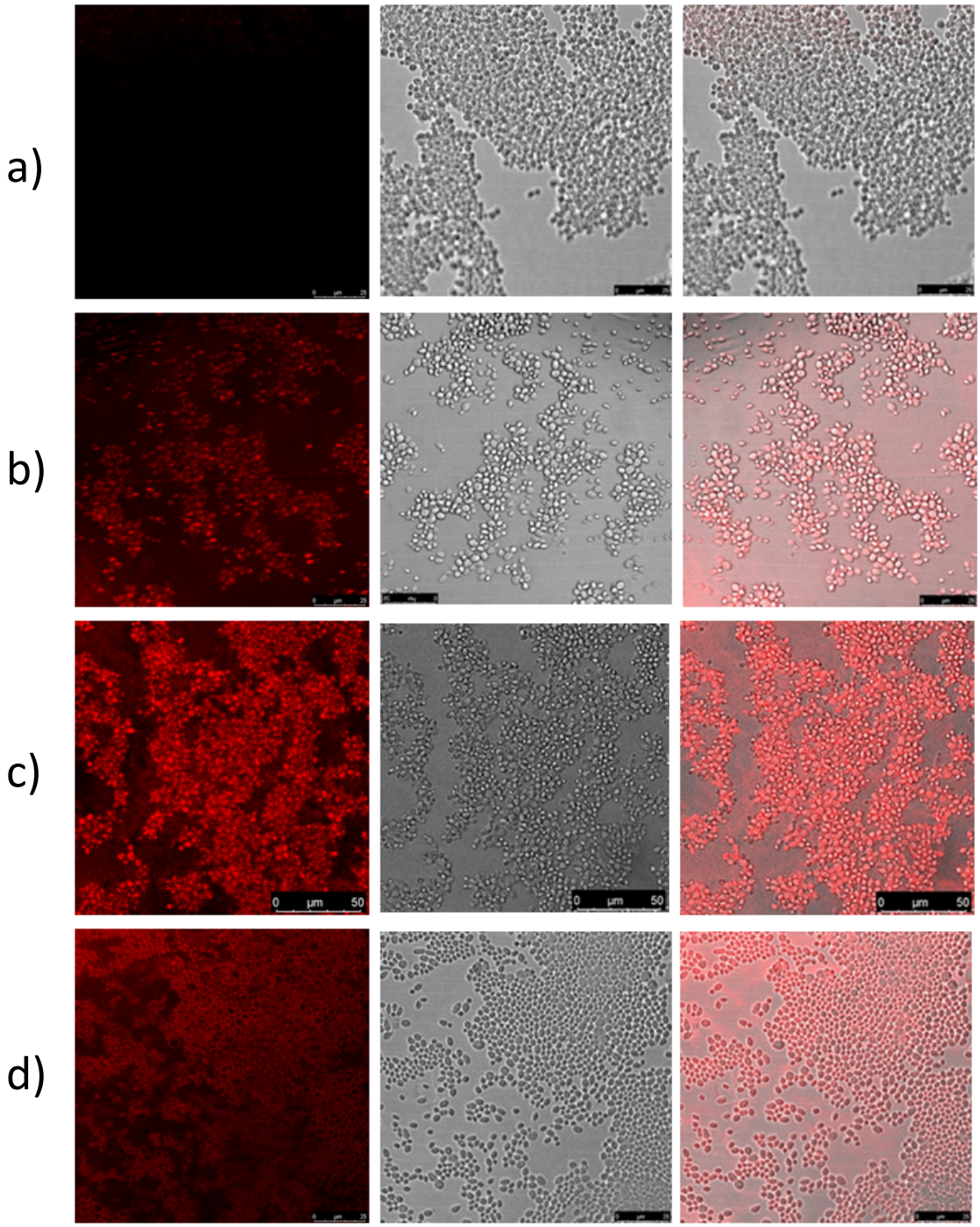


Figure 3.4 Fluorescence images of *S. cerevisiae* labeled cell culture.

Rows correspond to the following metabolic probes: a) unlabeled; b) **3.1**; c) **3.2**; d) **3.3**
Scale bars 25 µm, except c) 50 µm.

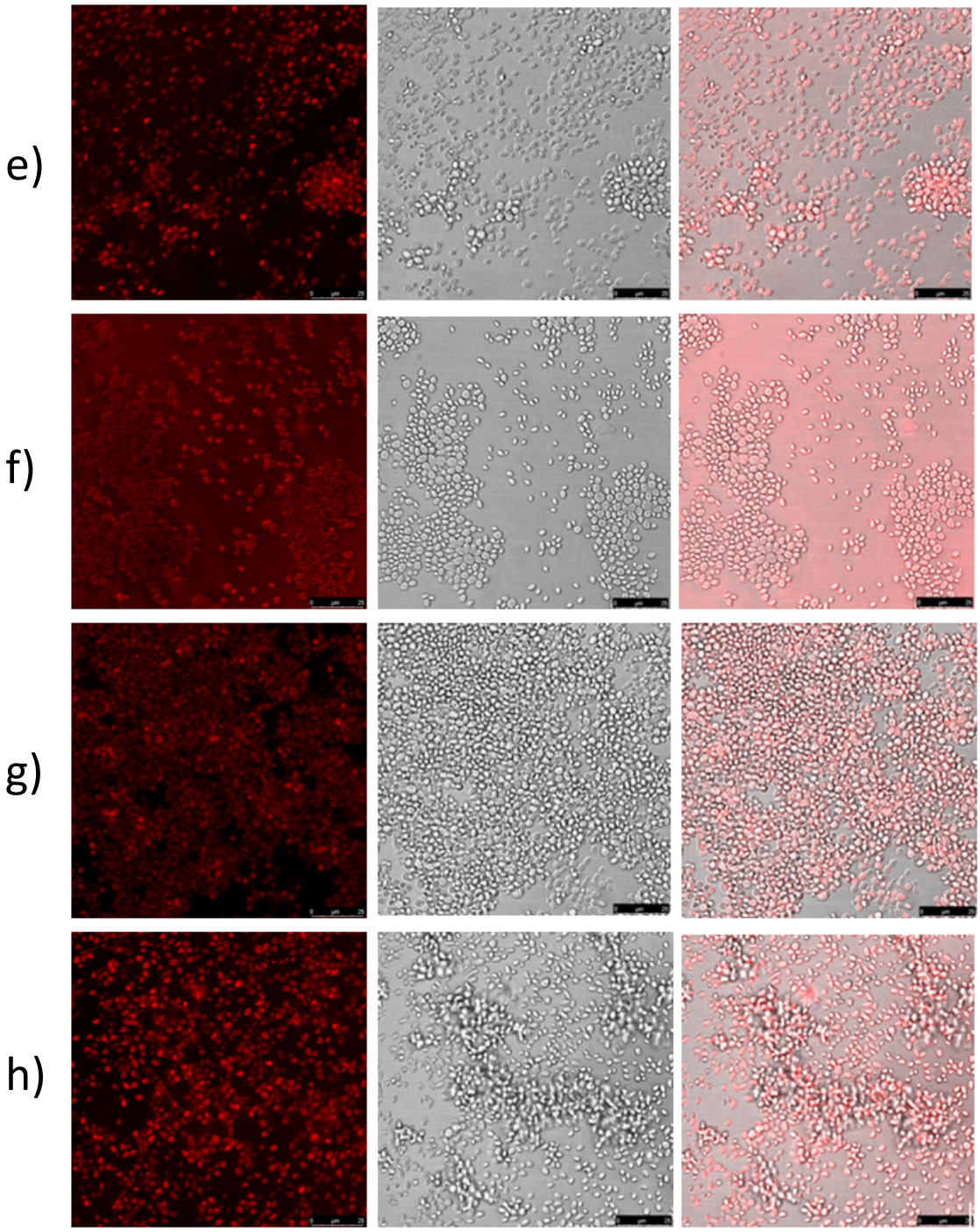


Figure 3.4 continued: Fluorescence images of S. cerevisiae labeled cell culture. Rows correspond to the following metabolic probes: e) **3.4**; f) **3.5**; g) **3.6**; h) **3.7** Scale bars 25 μm

fluorescence. This was corrected by increasing the number of steps of washing the cells with 20% DMSO in H_2O from 3 to 5 times to ensure all residual dye was successful removed. With this correction to the procedure, labeling of *S. cerevisiae* was visualized after the addition of probe **3.2** as can be seen in **Figure 3.3**. The top row of images shows control cells that were not treated with probe **3.2**, but were incubated with DBCO-Cy3, to evaluate background signal that does not result from metabolic labeling/click chemistry. Metabolically labeling samples treated with both probe and fluorescent reagents are shown in the bottom row of images. Image acquisition parameters such as zoom, z-position, and gain were maintained the same between samples to ensure accuracy. With the successful imaging of probe **3.2** by fluorescence microscopy, the remaining glycerol-N_3 and 3'-MAG-N_3 metabolic probes were ready for visualization via fluorescence microscopy.

Figure 3.4 shows the fluorescence microscopy images for probes **3.1** – **3.7**. The images are ordered A – H corresponding to each probes with row A as the control with no azide tagged probes added to the cell culture. Fluorescence, brightfield, and overlay images are included for each probe. All fluorescence images show successful labeling by metabolic incorporation of the azide labeled probes along with Cu-free click chemistry for attachment of the fluorescent tag. However, image F does appear to show a significant amount of background noise compared to the other images. All settings such as zoom, gain, and Z-position were maintained the same for each compound. It is possible that the image is slightly out of focus causing high background interference form the slide.

Residual background dye in the sample is also possible. Nevertheless, as addressed previously, the number of washing steps after incubation with the click dye was increased from 3 to 5 times to avoid this issue. Repetition of labeling with fluorescent click dye and image and subsequent imaging would be required to determine if these issue have caused the high background noise seen in image F.

Fluorescence TLC

With fluorescence microscopy validating metabolic labeling for probes **3.1** – **3.7**, subsequent studies of fluorescence TLC and tandem LC-MS were ready to analyze the probes. Fluorescence TLC experiments allow for the visualization of multiple labeled lipid species separated on an individual plate. Labeled lipid products will move differently on the TLC plate in comparison to their natural analog counterparts.[34] This is useful as new

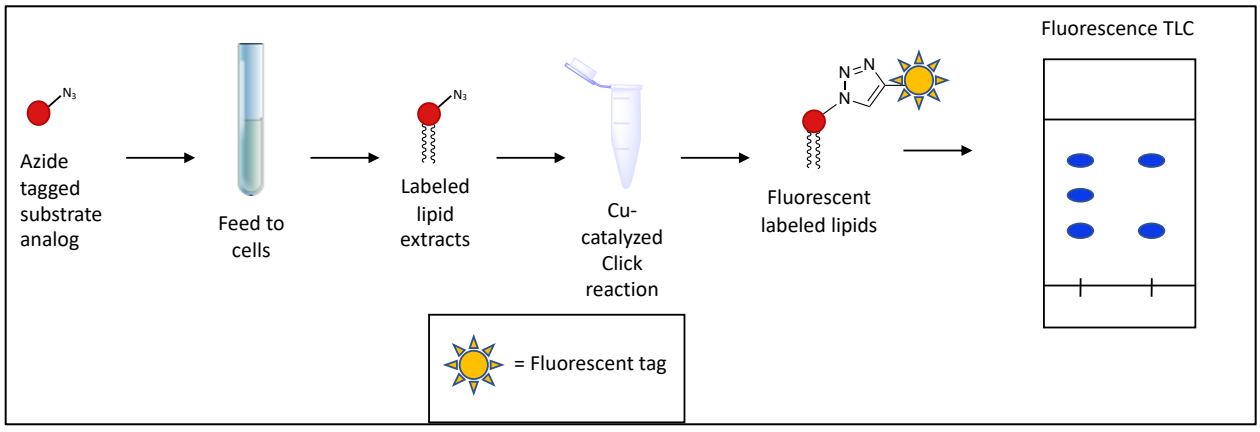


Figure 3.5 Overview of method for obtaining fluorescence TLC of metabolically labeled lipid extracts

spots on the TLC plate are an indication of successful metabolic labeling of downstream lipid products. However, newly labeled lipid products are expected to move similarly to incorporation of the fluorescent tag.

The labeled cells were processed to extract the lipids by first removing the proteins with MeOH. The lipids were then extracted with $CHCl_3$ and 0.1M AcOH in mQ H_2O. Copper catalyzed azide-alkyne cycloaddition was then used to click on the fluorescent tag. Plates developed with a solution of $CHCl_3$/MeOH/H_2O/AcOH (65:25:4:1) and stained with primulin to visualize by UV light. Initial results, shown in **Figure 3.6**, did not show the appearance of new spots. It is believed that an additional solvent system would be required in addition to a longer development time to achieve separation on the TLC plate.

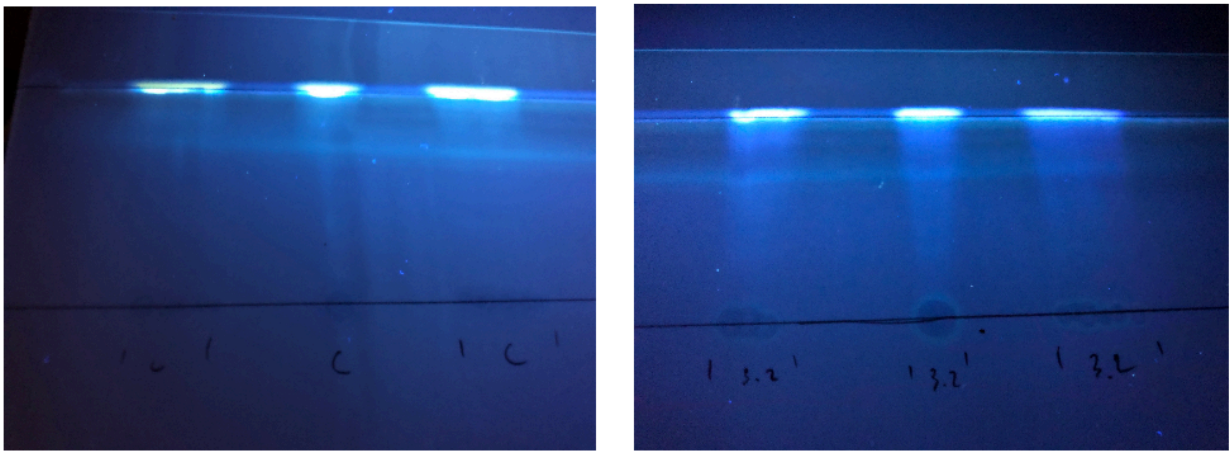


Figure 3.6 Initial fluorescence TLC images for unlabeled (left) and **3.2** (right)

3.3. Future Work

Further study of the probes discussed in this chapter is required for a more complete understanding of their effectiveness and application. While fluorescence TLC studies were initiated, more attempts are required to determine an appropriate solvent system for the separation of labeled lipid products. Initial results appear to show fluorescence but no separation of spots. This is most likely due to needing an additional solvent system and more developing time for better separation.

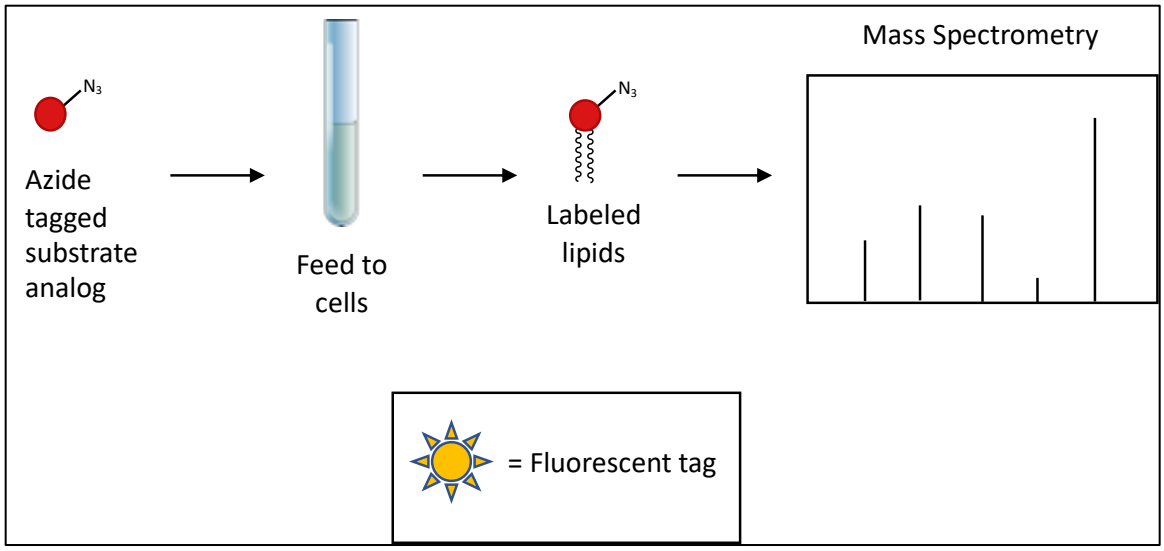


Figure 3.7 Overview of method for mass spectrometry analysis of azide tagged lipid extracts

Cell viability studies to determine the toxicity of probes at varying concentrations over a period of time would be valuable in differentiating between probe effectiveness. This could be completed in the same parameters as the original cell growth experiments.

However, optical density measurements would need to be taken at specified time intervals and increasing concentrations of each azide labeled metabolic probe would need to be used to ensure a proper distribution of toxicity data is achieved. Additionally, in vitro enzymatic assays could also be used to assess validation of labeling.

Mass spectrometry analysis by HPLC-MS/MS will also be used for identification and quantification of natural and azide tagged phospholipid and glycerolipid products. An overview of this process can be seen in **Figure 3.7**. Azide-tagged substrate analogs are fed to live cells where they are metabolically incorporated into the cell. These cells are then harvested, washed, and spun down to be used immediately or stored in the freezer at -80 °C for later use. Next, the proteins are isolated and removed from the labeled cells with MeOH. The lipids are then extracted using $CHCl_3$ and 0.1M AcOH in mQ H_2O. The labeled lipid extracts can be dried un $N_{2\ (g)}$ and are ready for mass spectrometry analysis. It is expected that a full spectrum of azide labeled lipid products will be detected including glycerolipids and phospholipids. Varying acyl carbon chain length and unsaturation will occur between lipids of the same species but can also be detected.

3.4. Experimental

Labeling *S. cerevisiae* with Azide-Tagged Probes and Cell Viability

Metabolic labeling experiments were performed in the laboratory of Dr. Todd Reynolds – Department of Microbiology, The University of Tennessee, Knoxville. *S.*

cerevisiae TRY 181 (WT, uraΔhisΔ) was streaked onto a yeast peptone dextrose (YPD) agar plate and incubated at 30 °C for 24 hours shaking at 300 rpm. A solution of 2% galactose minimal media was prepared with 6.7 g yeast nitrogen base (YNB) without amino acids, and 20 g galactose, 20 mg uracil, and 20 mg L-histidine added to enough mQ H_2O to produce 1000 mL of solution. After the additives were completely dissolved, the solution was placed in the autoclave for sterilization.[47] After incubation a loop of cells was inoculated into 5 mL of the 2% galactose minimal media solution in a glass tube with sterilized wooden rods and incubated overnight for approximately 31 hours at 30 °C with shaking at 300 rpm. An initial OD of the cell culture was measured and simple dilution values were calculated to reach a final OD of 0.8 with a total volume of solution of 5 mL. The cell culture was diluted into new glass tubes with fresh 2% galactose minimal media and spiked with the desired probe dissolved in EtOH with one tube spiked with an equal volume of EtOH as a control. These new cultures were incubated overnight for approximately 17 hours at 30 °C with shaking at 300 rpm. The OD was measured and recorded for each sample. The individual cultures were then spun at 3000 x g for 5 min at 4 °C. The cultures were then washed with 10 mL mQ H_2O and spun again at 3000 x g for 5 min at 4 °C. The supernatant was removed and the cultures were used immediately or stored at -80 °C.[45] For cell viability studies, the same procedure was followed but after the samples were spike with the appropriate probe, the OD of a culture sample was measured every 2 hours over a total 12 hour period and again at 24 hours to produce a growth curve.

Fluorescence Microscopy

After labeling *S. cerevisiae* with azide-tagged probes, cells were used immediately after harvesting or thawed on ice if using from storage at -80 °C. The cells were resuspended in 929 μL of mQ H_2O. The supernatant was then discarded and the cells were transferred to 2 mL Eppendorf tubes. Next, the cells were treated with 71 μL of the Cu-free click chemistry dye DBCO-Cy3 to reach a final concentration of 10 μM and incubated while shaking at room temperature for one hour. The cells were then centrifuged at 2500 rpm for 3 min and the dye solution was removed. The cell pellet was next washed with 1 mL of 20% DMSO in H_2O to removed residual dye, vortexed, and centrifuged at 2500 rpm for 3 min. This process was repeated 3 times, discarding the supernatant between each washing step. After the third wash, 1 mL of cold MeOH was added to remove any residual DMSO and the cells were incubated for 10 minutes at 0 °C. Upon completion of incubation, the cells were again centrifuged at 2500 rpm for 3 min and then the supernatant discarded. Finally, 1 mL of PBS solution (pH 7.4, 1.19 mM phosphates) was added to wash cells. The cells were centrifuged at 2500 rpm for 3 min and the supernatant was discarded.[45] The cells were resuspended in 200 μL of mQ water and 4 μL of the cell culture were fixed onto a slide and topped with a coverslip.[46] Slides were visualized and imaged immediately. Fluorescence microscopy imaging experiments were performed at the Advanced Microscopy and Imaging Center – The University of Tennessee, Knoxville

with the assistance of Dr. John Dunlap using a Leica SP8 White Light Laser Confocal System.

Lipid Extraction

After labeling *S. cerevisiae* with azide-tagged probes, cells were used immediately after harvesting or thawed on ice if using from storage at -80 °C. To extract the proteins, the cell pellet was resuspended in 300µL of cold PBS to which 600 µL of MeOH was added. The cells were then vortexed and 150 µL $CHCl_3$ was added. The cells were vortexed again and then placed into the centrifuge at 14,000 g for 5 minutes after which the supernatant was transferred to new Eppendorf tubes. Next, the lipid extraction was initiated by adding 300 µL of $CHCl_3$. The solution was vortexed after which 600µL of 0.1M AcOH in mQ H_2O was added and the mixture was again vortexed and placed into the centrifuge at 14,000 g for 5 minutes. The top aqueous layer was removed by aspiration and then using a pipet to remove any remaining aqueous layer. The bottom organic layer was then transferred to new Eppendorf tubes and the solvent was removed by slowly purging with N_2 for approximately 15 minutes. The extracted lipids were immediately resuspended in 8 µL of $CHCl_3$ or stored in the refrigerator overnight and resuspending the following day for analysis by TLC or MS.[48]

Fluorescence TLC Click Reaction

Once the lipids had successfully been extracted, 3.80 mg of Cu(I) was weighed out into an Eppendorf tube. To this was added 605 µL of MeCN and the solution was vortexed. Next, 6.8 µL of thawed naphthalimide dye (4-ethynyl-*N*-ethy-1,8-napthalimide) was placed into a separate tube and 200 µL of Cu(I)/ MeCN solution was added and vortexed. Subsequently, 30 µL of this freshly prepared solution was added to each lipid extract and the samples for vortexed and placed into the centrifuge at 14,000 g for 5 minutes. The samples were incubated in a water bath at 42 °C for 3 hours and then vortexed to mix and placed into the centrifuge at 14,000 g for 5 minutes. The samples were then applied to the TLC plate and developed with a solution of $CHCl_3$/MeOH/H_2O/AcOH 65:25:4:1. After developing, the plates were stained with primulin and visualized under UV light.[48]

REFERENCES

(1) Gruner, S. M. Intrinsic Curvature Hypothesis for Biomembrane Lipid Composition: A Role for Nonbilayer Lipids. *Proc. Natl. Acad. Sci. U. S. A.* **1985**, *82* (11), 3665–3669.

(2) Escribá, P. V.; Ozaita, A.; Ribas, C.; Miralles, A.; Fodor, E.; Farkas, T.; García-Sevilla, J. A. Role of Lipid Polymorphism in G Protein-Membrane Interactions: Nonlamellar-Prone Phospholipids and Peripheral Protein Binding to Membranes. *Proc. Natl. Acad. Sci. U. S. A.* **1997**, *94* (21), 11375–11380.

(3) Israelachvili, J.; Wennerström, H. Role of Hydration and Water Structure in Biological and Colloidal Interactions. *Nature*. Nature Publishing Group January 18, 1996, pp 219–225.

(4) Yáñez-Mó, M.; Siljander, P. R. M.; Andreu, Z.; Zavec, A. B.; Borràs, F. E.; Buzas, E. I.; Buzas, K.; Casal, E.; Cappello, F.; Carvalho, J.; et al. Biological Properties of Extracellular Vesicles and Their Physiological Functions. *J. of Extracell. Vesicles*. Co-Action Publishing 2015, pp 1–60.

(5) McNitt, C. D.; Popik, V. V.; Alves, D. S.; Best, M. D.; Alam, S.; Barrera, F. N.; Whitehead, S. A.; Bayer, A. M. A Clickable and Photocleavable Lipid Analogue for Cell Membrane Delivery and Release. *Bioconjug. Chem.* **2015**, *26* (6), 1021–1031.

(6) Kaneko, H.; Hosohara, M.; Tanaka, M.; Itoh, T. Lipid Composition of 30 Species of Yeast. *Lipids* **1976**, *11* (12), 837–844.

(7) Escribá, P. V.; González-Ros, J. M.; Goñi, F. M.; Kinnunen, P. K. J.; Vigh, L.; Sánchez-Magraner, L.; Fernández, A. M.; Busquets, X.; Horváth, I.; Barceló-Coblijn,

G. Membranes: A Meeting Point for Lipids, Proteins and Therapies: Translational Medicine. *J. Cell. Mol. Med.* **2008**, *12* (3), 829–875.

(8) Carrasco, S.; Mérida, I. Diacylglycerol, When Simplicity Becomes Complex. *Trends Biochem. Sci*. January 2007, pp 27–36.

(9) Danielli, J. F.; Davson, H. A Contribution to the Theory of Permeability of Thin Films. *J. Cell. Comp. Physiol.* **1935**, *5* (4), 495–508.

(10) Singer, S. J.; Nicolson, G. L. The Fluid Mosaic Model of the Structure of Cell Membranes. *Science (80-.).* **1972**, *175* (4023), 720–731.

(11) Simons, K.; Ikonen, E. Functional Rafts in Cell Membranes. *Nature*. Nature Publishing Group June 5, 1997, pp 569–572.

(12) Klug, L.; Daum, G. Yeast Lipid Metabolism at a Glance. *FEMS Yeast Res.* **2014**, *14* (3), 369–388.

(13) Fagone, P.; Jackowski, S. Membrane Phospholipid Synthesis and Endoplasmic Reticulum Function. *J. Lipid Res*. American Society for Biochemistry and Molecular Biology April 1, 2009, pp S311–S316.

(14) Gibellini, F.; Smith, T. K. The Kennedy Pathway-de Novo Synthesis of Phosphatidylethanolamine and Phosphatidylcholine. *IUBMB Life*. IUBMB Life June 2010, pp 414–428.

(15) De Kroon, A. I. P. M.; Rijken, P. J.; De Smet, C. H. Checks and Balances in Membrane Phospholipid Class and Acyl Chain Homeostasis, the Yeast Perspective. *Prog. Lipid Res*. Pergamon October 1, 2013, pp 374–394.

(16) Exton, J. H. Phosphatidylcholine Breakdown and Signal Transduction. *Biochi. Biophys. Acta.* Elsevier April 14, 1994, pp 26–42.

(17) Strahl, T.; Thorner, J. Synthesis and Function of Membrane Phosphoinositides in Budding Yeast, Saccharomyces Cerevisiae. *Biochim. Biophys Acta*. Elsevier March 1, 2007, pp 353–404.

(18) Vance, J. E.; Steenbergen, R. Metabolism and Functions of Phosphatidylserine. *Prog. Lipid Res*. Pergamon July 1, 2005, pp 207–234.

(19) Thormar, H.; Hilmarsson, H.; Bergsson, G. Stable Concentrated Emulsions of the 1-Monoglyceride of Capric Acid (Monocaprin) with Microbicidal Activities against the Food-Borne Bacteria Campylobacter Jejuni, Salmonella Spp., and Escherichia Coli. *Appl. Environ. Microbiol.* **2006**, *72* (1), 522–526.

(20) Isaacs, C. E.; Litov, R. E.; Thormar, H. Antimicrobial Activity of Lipids Added to Human Milk, Infant Formula, and Bovine Milk. *J. Nutr. Biochem.* **1995**, *6* (7), 362–366.

(21) Drake, D. R.; Brogden, K. A.; Dawson, D. V.; Wertz, P. W. Thematic Review Series: Skin Lipids - Antimicrobial Lipids at the Skin Surface. *J. Lipid Res*. American Society for Biochemistry and Molecular Biology January 1, 2008, pp 4–11.

(22) Brogden, N. K.; Mehalick, L.; Fischer, C. L.; Wertz, P. W.; Brogden, K. A. The Emerging Role of Peptides and Lipids as Antimicrobial Epidermal Barriers and Modulators of Local Inflammation. *Skin Pharmacol. Phys*. Karger Publishers June 2012, pp 167–181.

(23) Foster, D. A. Phosphatidic Acid Signaling to MTOR: Signals for the Survival of Human Cancer Cells. *Biochim. Biophys. Acta - Mol. Cell Biol. Lipids* **2009**, *1791* (9), 949–955.

(24) Castellano, E.; Downward, J. RAS Interaction with PI3K: More Than Just Another Effector Pathway. *Genes Cancer* **2011**, *2* (3), 261–274.

(25) Klein, S.; Heinzle, E. Isotope Labeling Experiments in Metabolomics and Fluxomics. *Wiley Interdiscip. Rev. Syst. Biol. Med.* **2012**, *4* (3), 261–272.

(26) Buchberger, A. R.; DeLaney, K.; Johnson, J.; Li, L. Mass Spectrometry Imaging: A Review of Emerging Advancements and Future Insights. *Anal. Chem*. American Chemical Society January 2, 2018, pp 240–265.

(27) Jacobs, C. L.; Yarema, K. J.; Mahal, L. K.; Nauman, D. A.; Charters, N. W.; Bertozzi, C. R. Metabolic Labeling of Glycoproteins with Chemical Tags through Unnatural Sialic Acid Biosynthesis. *Methods Enzymol.* **2000**, *327*, 260–275.

(28) Kolb, H. C.; Finn, M. G.; Sharpless, K. B. Click Chemistry: Diverse Chemical Function from a Few Good Reactions. *Angew. Chemie Int. Ed.* **2001**, *40* (11), 2004–2021.

(29) Hein, J. E.; Fokin, V. V. Copper-Catalyzed Azide-Alkyne Cycloaddition (CuAAC) and beyond: New Reactivity of Copper(i) Acetylides. *Chem. Soc. Rev.* **2010**, *39* (4), 1302–1315.

(30) Saxon, E.; Armstrong, J. I.; Bertozzi, C. R. A “Traceless” Staudinger Ligation for the Chemoselective Synthesis of Amide Bonds. *Org. Lett.* **2000**, *2* (14), 2141–2143.

(31) Jao, C. Y.; Roth, M.; Welti, R.; Salic, A. Metabolic Labeling and Direct Imaging of Choline Phospholipids in Vivo. *Proc. Natl. Acad. Sci. U. S. A.* **2009**, *106* (36), 15332–15337.

(32) Jao, C. Y.; Roth, M.; Welti, R.; Salic, A. Biosynthetic Labeling and Two-Color Imaging of Phospholipids in Cells. *ChemBioChem* **2015**, *16* (3), 472–476.

(33) Jao, C. Y.; Nedelcu, D.; Lopez, L. V.; Samarakoon, T. N.; Welti, R.; Salic, A. Bioorthogonal Probes for Imaging Sterols in Cells. *ChemBioChem* **2015**, *16* (4), 611–617.

(34) Thiele, C.; Papan, C.; Hoelper, D.; Kusserow, K.; Gaebler, A.; Schoene, M.; Piotrowitz, K.; Lohmann, D.; Spandl, J.; Stevanovic, A.; et al. Tracing Fatty Acid Metabolism by Click Chemistry. *ACS Chem. Biol.* **2012**, *7* (12), 2004–2011.

(35) Gaebler, A.; Milan, R.; Straub, L.; Hoelper, D.; Kuerschner, L.; Thiele, C. Alkyne Lipids as Substrates for Click Chemistry-Based in Vitro Enzymatic Assays. *J. Lipid Res.* **2013**, *54* (8), 2282–2290.

(36) Lu, L.; Gao, J.; Guo, Z. Labeling Cell Surface GPIs and GPI-Anchored Proteins through Metabolic Engineering with Artificial Inositol Derivatives. *Angew. Chemie Int. Ed.* **2015**, *54* (33), 9679–9682.

(37) Bumpus, T. W.; Baskin, J. M. A Chemoenzymatic Strategy for Imaging Cellular Phosphatidic Acid Synthesis. *Angew. Chemie Int. Ed.* **2016**, *55* (42), 13155–13158.

(38) Ricks, T. J.; Cassilly, C. D.; Carr, A. J.; Alves, D. S.; Alam, S.; Tscherch, K.; Yokley, T. W.; Workman, C. E.; Morrell-Falvey, J. L.; Barrera, F. N.; et al. Labeling of

Phosphatidylinositol Lipid Products in Cells through Metabolic Engineering by Using a Clickable Myo-Inositol Probe. *ChemBioChem* **2019**, *20* (2), 172–180.

(39) Lykidis, A. Comparative Genomics and Evolution of Eukaryotic Phospholipid Biosynthesis. *Prog. Lipid Res*. Pergamon May 1, 2007, pp 171–199.

(40) Smith, M. D.; Sudhahar, C. G.; Gong, D.; Stahelin, R. V.; Best, M. D. Modular Synthesis of Biologically Active Phosphatidic Acid Probes Using Click Chemistry. *Mol. Biosyst.* **2009**, *5* (9), 962–972.

(41) Bouzide, A.; Sauvé, G. Silver(I) Oxide Mediated Highly Selective Monotosylation of Symmetrical Diols. Application to the Synthesis of Polysubstituted Cyclic Ethers. *Org. Lett.* **2002**, *4* (14), 2329–2332.

(42) Tanaka, T.; Tamatsukuri, S.; Ikehara, M. New Approach to the Synthesis of Deoxynucleoside-Phosphoramidite Derivatives. *Tetrahedron Lett.* **1986**, *27* (2), 199–202.

(43) Dreef, C. E.; Tuinman, R. J.; Lefeber, A. W. M.; Elie, C. J. J.; van der Marel, G. A.; van Boom, J. H. Synthesis of Racemic 3-Methylphosphonate Analogues of Myo-Inositol 3,4-Bis- and 1,3,4-Trisphosphate. *Tetrahedron* **1991**, *47* (26), 4709–4722.

(44) Carr, A. *Synthesis and Application of Biomimetic Probes for Investigating Protein-Lipid Interactions and Lipid Metabolism*; The University of Tennessee, Knoxville, 2018.

(45) Alam, S. *Development of New Methods for Liposomal Drug Delivery and the Labeling of Cellular Lipids*; The University of Tennessee, Knoxville, 2016.

(46) Ricks, T. *Design and Synthesis of Analogs of Myo-Inositol, Serine, and Cysteine to Enable Chemical Biology Studies*; The University of Tennessee, Knoxville, 2017.

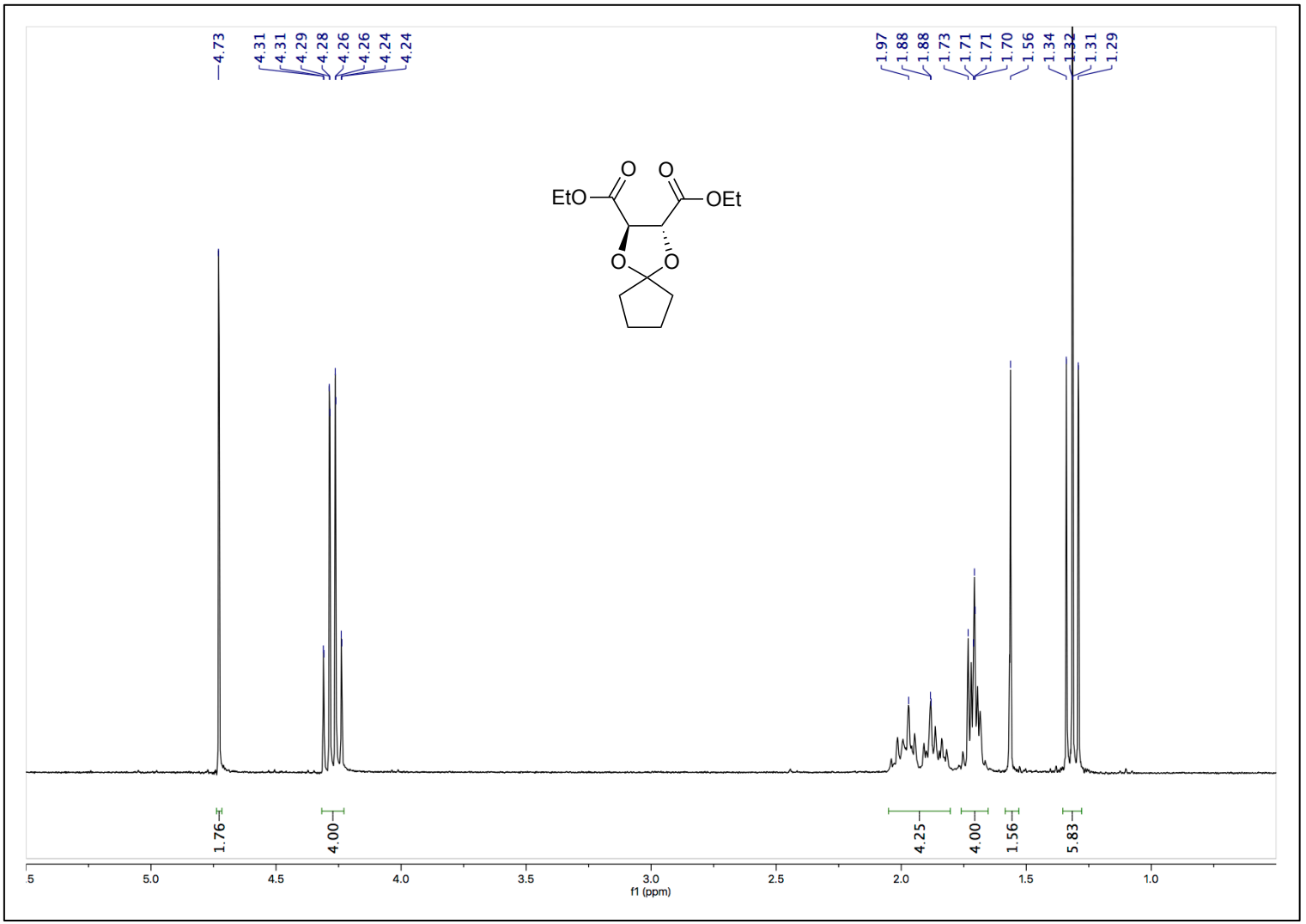
(47) Jesch, S. A.; Zhao, X.; Wells, M. T.; Henry, S. A. Genome-Wide Analysis Reveals Inositol, Not Choline, as the Major Effector of Ino2p-Ino4p and Unfolded Protein Response Target Gene Expression in Yeast. *J. Biol. Chem.* **2005**, *280* (10), 9106–9118.

(48) Haberkant, P.; Stein, F.; Höglinger, D.; Gerl, M. J.; Brügger, B.; Van Veldhoven, P. P.; Krijgsveld, J.; Gavin, A.-C.; Schultz, C. Bifunctional Sphingosine for Cell-Based Analysis of Protein-Sphingolipid Interactions. *ACS Chem. Biol.* **2016**, *11* (1), 222–230.

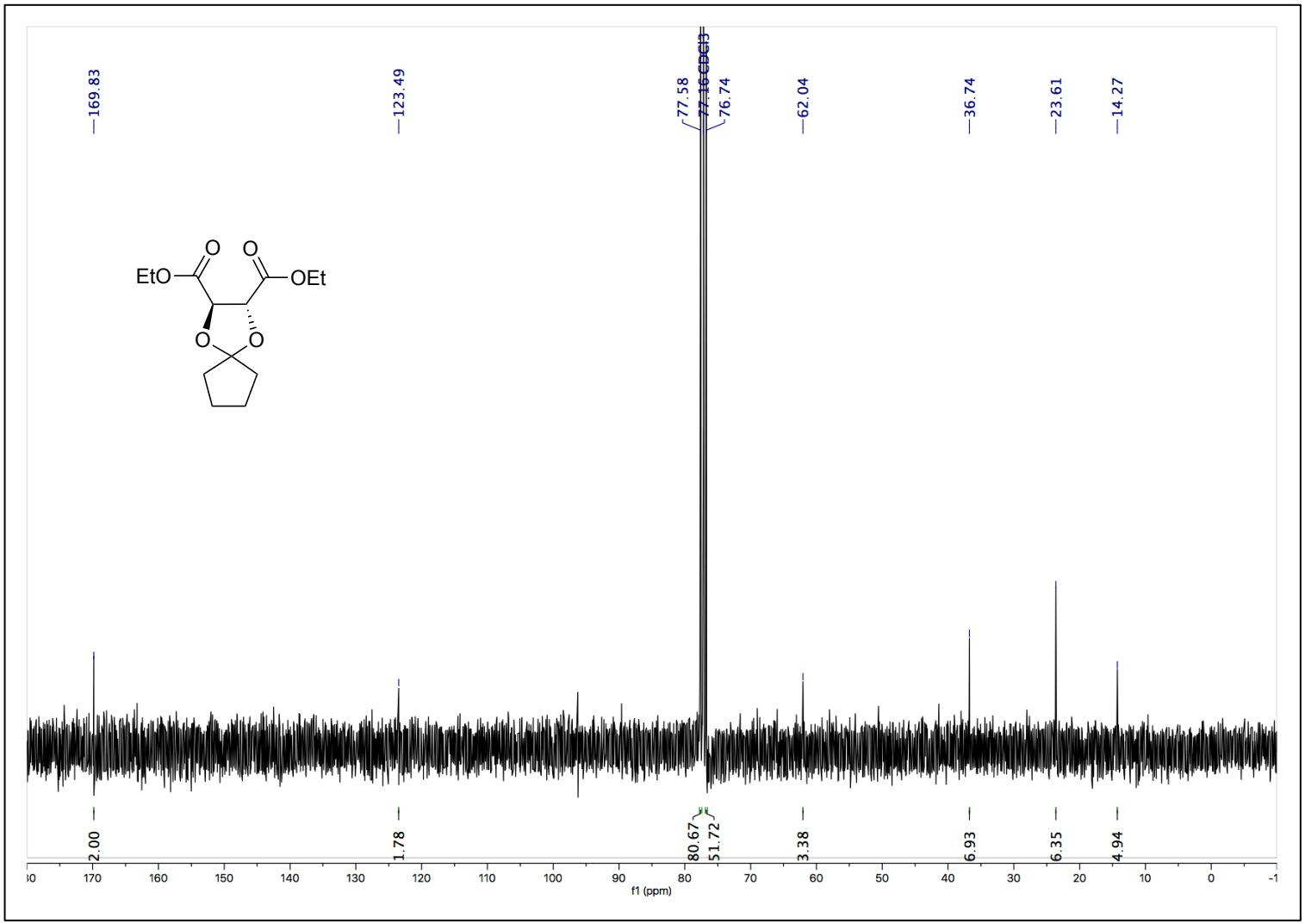
APPENDIX

NMR SPECTRA

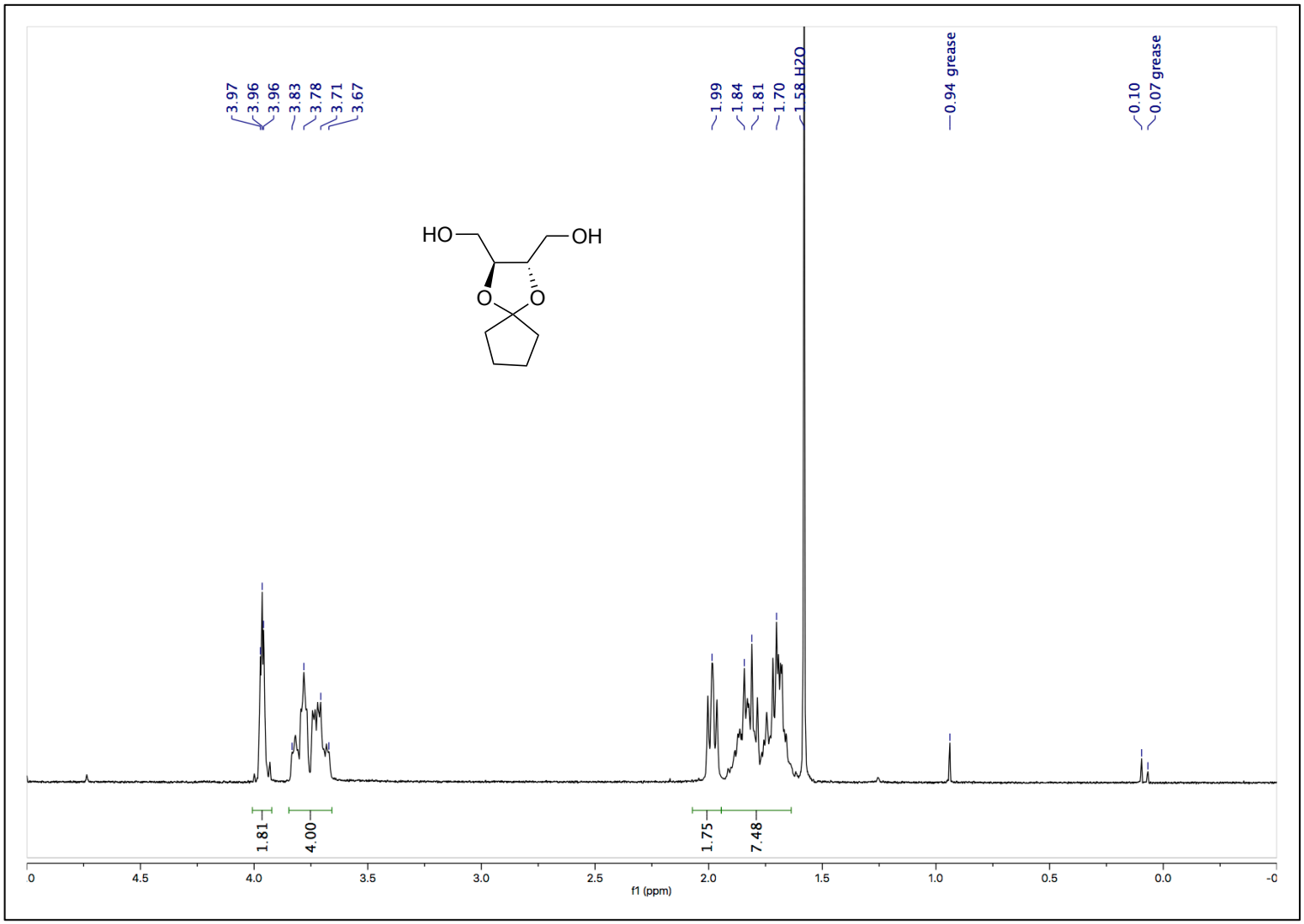
^{1}H NMR (300 MHz, CDCl3) of compound **2.4**



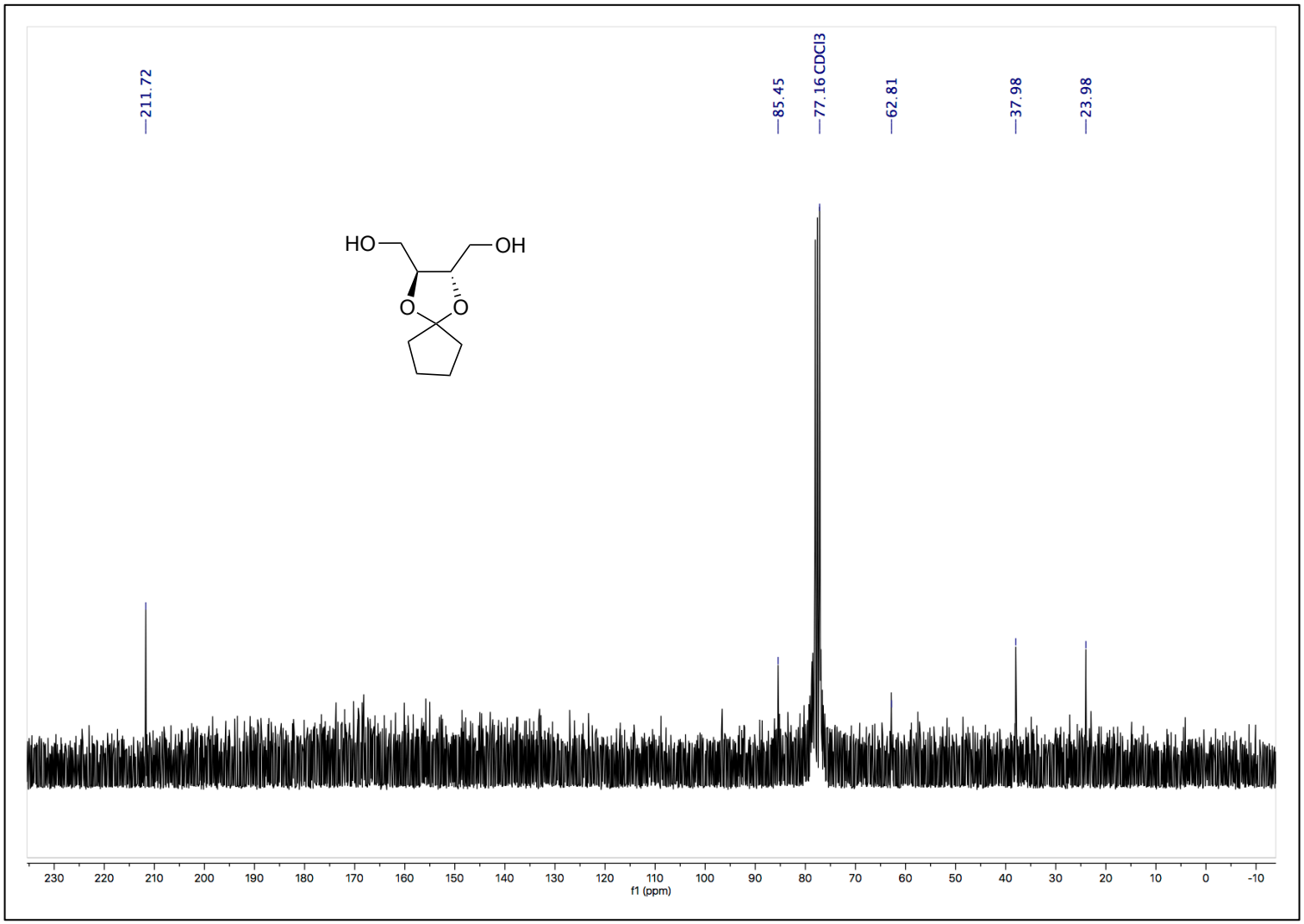
^{13}C NMR (75 MHz, CDCl3) of compound **2.4**



^{1}H NMR (300 MHz, CDCl3) of compound **2.5**

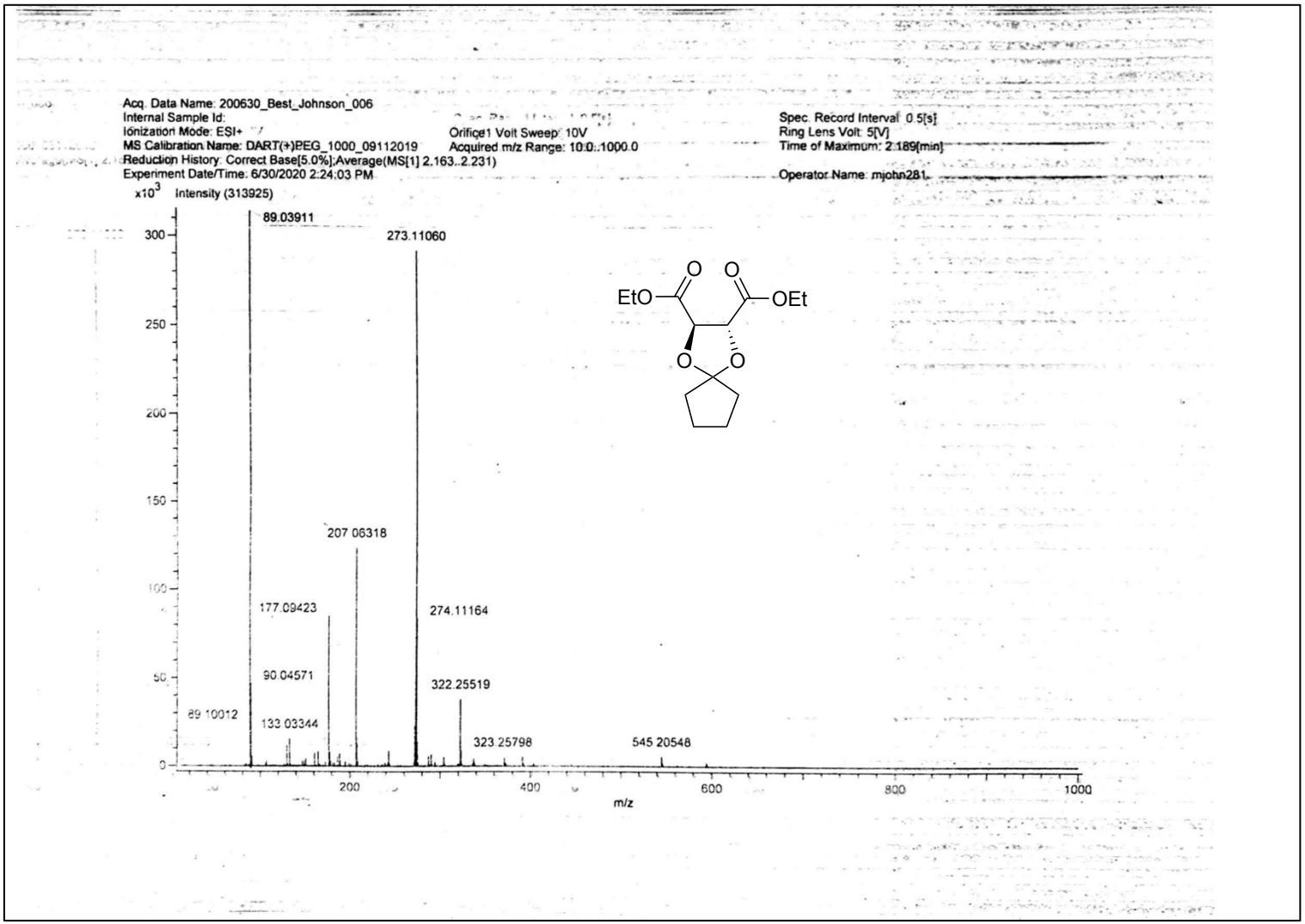


^{13}C NMR (75 MHz, CDCl3) of compound **2.5**

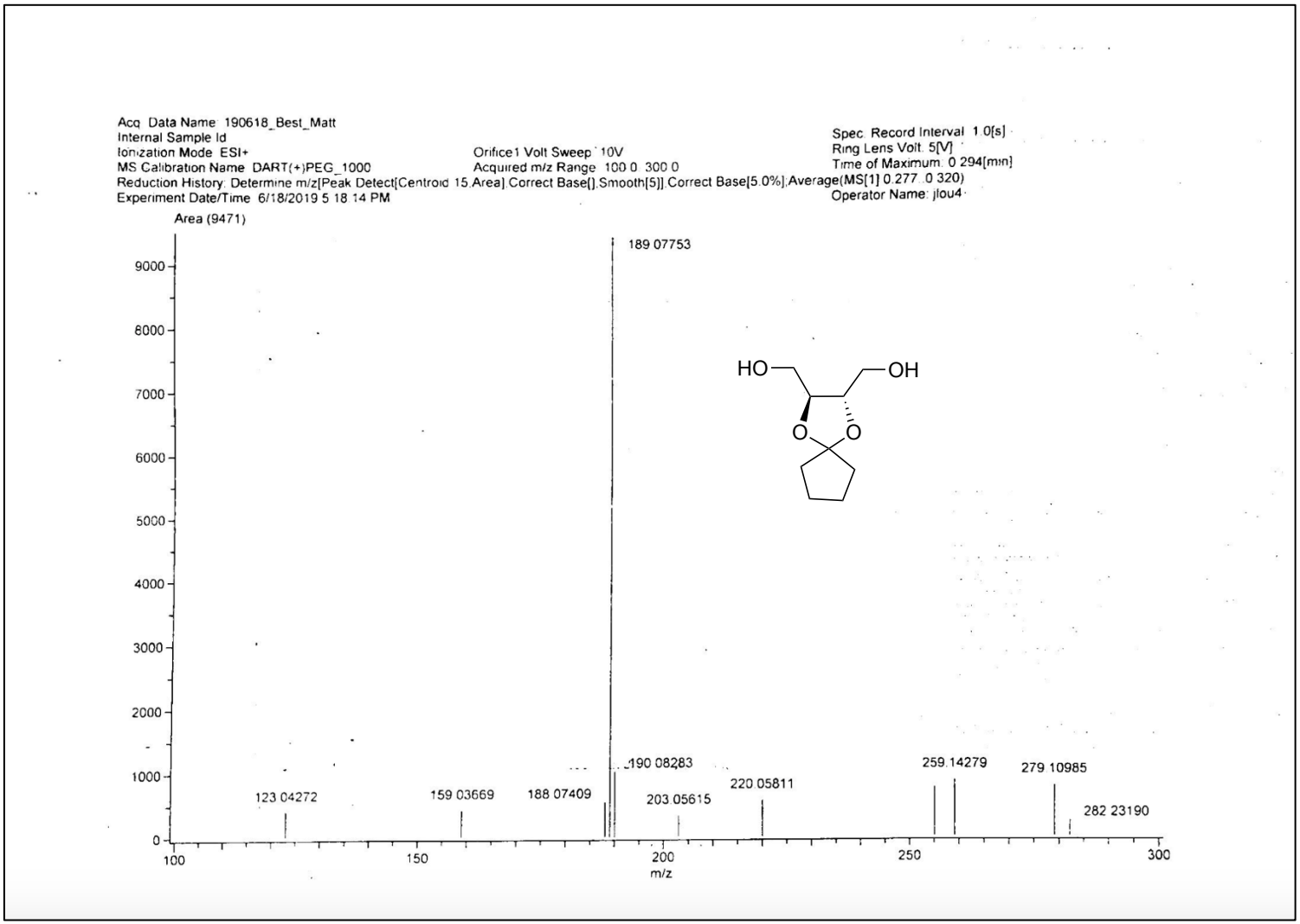


HIGH RESOLUTION MASS SPECTRA

ACCUTOF-DART Mass Spectrum of compound **2.4**



ACCUTOF-DART Mass Spectrum of compound **2.5**



VITA

Matthew R. Johnson was born in Hanover, IN. There, he developed a love for chemistry from his father, Richard Johnson, and his high school chemistry teacher, Mickey Waller. He enrolled at Brigham Young University where he began his collegiate studies in Chemical Engineering. While at BYU, Matthew served a two year mission for The Church of Jesus Christ of Latter-Day Saints in Santiago, Chile. Upon returning, he chose to explore other majors, finally deciding on Biochemistry. In conjunction with changing majors, he also choose to transfer to Utah Valley University where his wife Gina was working full time for their MBA program. During his time at UVU he developed a passion for organic chemistry and worked under the guidance of Dr. Stephen Chamberland on total synthesis of the natural products phidianidines A & B and clavatadine B. His work on the clavatadine B project was presented at the National Meeting of the American Chemical Society in New Orleans, LA in 2018. It was during this period of research that Matthew felt drawn to pursue a graduate degree and further his studies. Matthew graduated from Utah Valley University in August 2018 and enrolled at the University of Tennessee-Knoxville that same year. Here he joined the research group of Dr. Michael Best to pursue studies in organic synthesis and chemical biology working toward a Master of Science in Organic Chemistry.